References

[1] F. Radu and J. Sánchez-Barriga, *Ferrimagnetic Heterostructures for Applications in Magnetic Recording* (Elsevier, Amsterdam, Netherlands, 2018).

[2] J. A. González, J. P. Andrés, and R. L. Antón, *Applied Trends in Magnetic Rare Earth/Transition Metal Alloys and Multilayers*, Sensors **21**, 1 (2021).

[3] M. N. Baibich, J. M. Broto, A. Fert, F. N. Van Dau, F. Petroff, P. Eitenne, G. Creuzet, A. Friederich, and J. Chazelas, *Giant Magnetoresistance of (001)Fe/(001)Cr Magnetic Superlattices*, Phys. Rev. Lett. **61**, 2472 (1988).

[4] D. Weller and A. Moser, *Thermal Effect Limits in Ultrahigh-Density Magnetic Recording*, IEEE Trans. Magn. **35**, 4423 (1999).

[5] P. M. Enriquez-Navas and M. L. Garcia-Martin, *Application of Inorganic Nanoparticles for Diagnosis Based on MRI*, 1st ed., Vol. 4 (Elsevier LTD., 2012).

[6] V. Marghussian, *Magnetic Properties of Nano-Glass Ceramics* (2015).

[7] T. D. Clemons, R. H. Kerr, and A. Joos, *Multifunctional Magnetic Nanoparticles: Design, Synthesis, and Biomedical Applications*, Vols. 1–5 (Elsevier Ltd., 2019).

[8] M. Yu, M. F. Doemer, and D. J. Sellmyer, *Thermal Stability and Nanostructure of CoCrPt Longitudinal Recording Media*, IEEE Trans. Magn. **34**, 1534 (1998).

[9] J. Sayama, K. Mizutani, T. Asahi, and T. Osaka, *Thin Films of SmCo5 with Very High Perpendicular Magnetic Anisotropy*, Appl. Phys. Lett. **85**, 5640 (2004).

[10] S. M. Na, S. J. Sun, and S. H. Lima, *Fabrication Condition Effects on the Magnetic and Magnetostrictive Properties of Sputtered Tb-Fe Thin Films*, J. Appl. Phys. **93**, 8507 (2003).

[11] B. Brahma, R. Hussain, R. K. Basumatary, Aakansha, S. Ravi, R. Brahma, and S. K. Srivastava, *Influence of Cu Insertion Layer on Magnetic Properties of Co-Tb/Cu/Co-Tb Thin Films*, J. Supercond. Nov. Magn. **33**, 2891 (2020).

[12] K. Ueda, M. Mann, C. Pai, A. Tan, G. S. D. Beach, K. Ueda, M. Mann, C. Pai, A. Tan, and G. S. D. Beach, *Magnetic Anisotropy Spin-Orbit Torques in Ta/TbxCo1001-x Ferrimagnetic Alloy Films with Bulk Perpendicular Magnetic Anisotropy*, Appl. Phys. Lett. **109**, 232403 (2016).

[13] M. Ohta, K. Yamada, Y. Satake, A. Fujita, and K. Fukamichi, *Origin of Perpendicular Magnetic Anisotropy in Tb-Fe Amorphous Alloy*, Mater. Trans. **44**, 2605 (2003).

[14] X. J. Liu, C. Song, F. Zeng, X. B. Wang, and F. Pan, *Influence of Annealing on Microstructure and Magnetic Properties of Co-Sputtered Co-Doped ZnO Thin Films*, J. Phys. D. Appl. Phys. **40**, 1608 (2007).

[15] T. Katayama, K. Hasegawa, K. Kawanishi, and T. Tsushima, *Annealing Effects on Magnetic Properties of Amorphous GdCo, GdFe, and GdCoMo Films*, J. Appl. Phys. **49**, 1759 (1978).

[16] H. C. Jiang, W. L. Zhang, W. X. Zhang, and B. Peng, *Effects of Argon Pressure on Magnetic Properties and Low-Field Magnetostriction of Amorphous TbFe Films*, Phys. B Condens. Matter **405**, 834 (2010).

[17] W. Pauli, *The Connection between Spin and Statistics*, Phys. Rev. **58**, 716 (1940).

[18] M. Massimi, *Pauli's Exclusion Principle The Origin and Validation of a Scientific Principle* (CAMBRIDGE UNIVERSITY PRESS, New York, 2005).

[19] J. M. D. Coey, *Magnetism and Magnetic Materials*, 1st Editio (CAMBRIDGE UNIVERSITY PRESS, Dublin, 2009).

[20] M. Getzlaff, *Fundamentals of Magnetism* (Springer, New York, 2008).

[21] C. Kettel, *Introduction to Solid State Physics*, 8th ed. (John Wiley & Sons, Berkeley, USA, 2005).

[22] M. L. Yan, N. Powers, and D. J. Sellmyer, *Highly Oriented Nonepitaxially Grown L10 FePt Films*, J. Appl. Phys. **93**, 8292 (2003).

[23] W. P. Wolf, *Ferrimagnetism*, Reports Prog. Phys. **24**, 212 (1961).

[24] L. Neel, *Antiferromagnetism and Ferrimagnetism*, Proc. Phys. Soc. **65**, 869 (1952).

[25] D. Azuma, *Magnetic Materials*, Vol. 7 (Elsevier Ltd., 2018).

[26] N. Kostevšek and I. Serša, *Characterization of Metal-Based Nanoparticles as Contrast Agents for Magnetic Resonance Imaging*, Compr. Anal. Chem. **93**, 303 (2021).

[27] P. J. Grundy, *Magnetic Layers: Anisotropy*, Encycl. Mater. Sci. Technol. 4788 (2001).

[28] A. J. Freeman, H. Krakauer, S. Ohnishi, D. sheng Wang, M. Weinert, and E. Wimmer, *Magnetism At Surfaces and Interfaces.*, Vol. 43 (Academic Press, 1982).

[29] H. Gao, T. Harumoto, W. Luo, R. Lan, H. Feng, Y. Du, Y. Nakamura, and J. Shi, *Room Temperature Perpendicular Exchange Bias in CoNi/(Co,Ni)O Multilayers with Perpendicular Magnetic Anisotropy Directly Induced by FM/AFM Interface*, J. Magn. Magn. Mater. **473**, 490 (2019).

[30] N. Y. Schmidt, S. Laureti, F. Radu, H. Ryll, C. Luo, F. D'Acapito, S. Tripathi, E. Goering, D. Weller, and M. Albrecht, *Structural and Magnetic Properties of FePt-Tb Alloy Thin Films*, Phys. Rev. B **100**, 1 (2019).

[31] B. Brahma, R. Hussain, Aakansha, P. Behera, S. Ravi, R. Brahma, and S. K. Srivastava, *Tuning the Perpendicular Magnetic Anisotropy of [Co(0.3nm)/Ni(0.6nm)]20 Multilayer Thin Films*, Thin Solid Films **728**, 0 (2021).

[32] C. Brombacher, H. Schletter, M. Daniel, P. Matthes, N. Jöhrmann, M. Maret, D. Makarov, M. Hietschold, and M. Albrecht, *FePtCu Alloy Thin Films: Morphology, $L1_0$ Chemical Ordering, and Perpendicular Magnetic Anisotropy*, J. Appl. Phys. **112**, (2012).

[33] R. Hussain, Aakansha, B. Brahma, R. Basumatary, R. Brahma, S. Ravi, and S. K. Srivastava, *Magnetic Property of Thin Film of Co-Tb Alloys Deposited on the Barrier Layer of Ordered Anodic Alumina Templates*, J. Supercond. Nov. Magn. **33**, 1759 (2020).

[34] D. Wu, S. Chen, Z. Zhang, B. Ma, and Q. Y. Jin, *Enhancement of Perpendicular Magnetic Anisotropy in Co/Ni Multilayers by in Situ Annealing the Ta/Cu under-Layers*, Appl. Phys. Lett. **103**, 242401 (2013).

[35] L. You, R. C. Sousa, S. Bandiera, B. Rodmacq, and B. Dieny, *Co/Ni Multilayers with Perpendicular Anisotropy for Spintronic Device Applications*, Appl. Phys. Lett. **100**, 1 (2012).

[36] N. A. Frey, S. Srinath, H. Srikanth, M. Varela, S. Pennycook, G. X. Miao, and A. Gupta, *Magnetic Anisotropy in Epitaxial CrO_2 and CrO_2/Cr_2O_3 Bilayer Thin Films*, Phys. Rev. B - Condens. Matter Mater. Phys. **74**, 1 (2006).

[37] Y. Ding, J. H. Judy, and J. P. Wang, *[CoFe/Pt]×n Multilayer Films with a Small Perpendicular Magnetic Anisotropy*, J. Appl. Phys. **97**, 1 (2005).

[38] S. Mangin et al., *Engineered Materials for All-Optical Helicity-Dependent Magnetic Switching*, Nat. Mater. **13**, 286 (2014).

[39] P. Hansen, C. Clausen, G. Much, M. Rosenkranz, and K. Witter, *Magnetic and Magneto-Optical Properties of Rare-Earth Transition-Metal Alloys Containing Gd, Tb, Fe, Co*, J. Appl. Phys. **66**, 756 (1989).

[40] P. Hansen, S. Klahn, C. Clausen, G. Much, and K. Witter, *Magnetic and Magneto-Optical Properties of Rare-Earth Transition-Metal Alloys Containing Dy, Ho, Fe, Co*, J. Appl. Phys. **69**, 3194 (1991).

[41] N. Heiman and K. Lee, *Magnetic Properties of Ho-Co and Ho-Fe Amorphous Films*, Phys. Rev. Lett. **33**, 778 (1974).

[42] Y. Suzuki, S. Takayama, F. Kirino, and N. Ohta, *Single Ion Model for Perpendicular Magnetic Anisotropy in RE-TM Amorphous Films*, IEEE Trans. Magn. **MAG-23**, 2275 (1987).

[43] N. Heiman, N. Kazama, D. F. Kyser, and V. J. Minkiewicz, *Effects of Substrate Bias and Annealing on the Properties of Amorphous Alloy Films of Gd-Co, Gd-Fe, and Gd-Co-X (X=Mo,Cu,Au)*, J. Appl. Phys. **49**, 366 (1978).

[44] P. Chaudhari, J. J. Cuomo, and R. J. Gambino, *Amorphous Metallic Films for Bubble Domain Applications*, IBM J. Res. Dev. **17**, 66 (1973).

[45] T. Mizoguchi and G. S. Cargill, *Magnetic Anisotropy from Dipolar Interactions in Amorphous Ferrimagnetic Alloys*, J. Appl. Phys. **50**, 3570 (1979).

[46] R. J. Gambino and J. J. Cuomo, *Selective Resputtering-Induced Anisotropy in*

Amorphous Films., J. Vac. Sci. Technol. **15**, 296 (1978).

[47] H. Takagi, S. Tsunashima, S. Uchiyama, and T. Fujii, *Stress Induced Anisotropy in Amorphous Gd-Fe and Tb-Fe Sputtered Films*, J. Appl. Phys. **50**, 1642 (1979).

[48] S. Yoshino, H. Takagi, S. Tsunashima, M. Masuda, and S. Uchiyama, *Perpendicular Magnetic Anisotropy of Tbco Films*, Jpn. J. Appl. Phys. **23**, 188 (1984).

[49] S. Tsunashima, K. Kamegaki, T. Fujii, and S. Uchiyama, *Magnetoelastic Contribution to Perpendicular Anisotropy in Amorphous Gd-Co and Gd-Fe Films*, IEEE Trans. Magn. **MAG-14**, 844 (1978).

[50] M. Ding and S. J. Poon, *Tunable Perpendicular Magnetic Anisotropy in GdFeCo Amorphous Films*, J. Magn. Magn. Mater. **339**, 51 (2013).

[51] C. Lee, L. Ye, J. Lee, W. Chen, C. Huang, G. Chern, and T. Wu, *Ultrathin (Gd , Tb) -FeCo Films With Perpendicular Magnetic Anisotropy*, IEEE Trans. Magn. **45**, 3808 (2009).

[52] K. Ohashi, H. Takagi, S. Tsunashima, S. Uchiyama, and T. Fujii, *Magnetic Aftereffect Due to Domain Wall Motion in Amorphous Tb-Fe Sputtered Films*, J. Appl. Phys. **50**, 1611 (1979).

[53] F. Rio, P. Bernstein, and M. Labrune, *Magnetization Process in RE-TM Alloys: Wall Mobility and Nucleation*, IEEE Trans. Magn. **MAG-23**, 2266 (1987).

[54] M. Labrune, S. Andrieu, F. Rio, and P. Bernstein, *Time Dependence of the Magnetization Process of RE-TM Alloys*, J. Magn. Magn. Mater. **80**, 211 (1989).

[55] A. Lyberatos, J. Earl, and R. W. Chantrell, *Model of Thermally Activated Magnetization Reversal in Thin Films of Amorphous Rare-Earth-Transition-Metal Alloys*, Phys. Rev. B **53**, 5493 (1996).

[56] T. H. Pham et al., *Thermal Contribution to the Spin-Orbit Torque in Metallic-Ferrimagnetic Systems*, Phys. Rev. Appl. **9**, 064032 (2018).

[57] J. Swerts, K. Temst, M. J. Van Bael, C. Van Haesendonck, and Y. Bruynseraede, *Magnetic Domain Wall Trapping by In-Plane Surface*

Roughness Modulation, Appl. Phys. Lett. **82**, 1239 (2003).

[58] C. E. Davies, R. E. Somekh, and J. E. Evetts, *Magnetic Properties of Sputter-Deposited Amorphous Rare Earth-Transition Metal Thin Films*, Vacuum **38**, 797 (1988).

[59] H. Basumatary, J. Arout Chelvane, D. V. Sridhara Rao, S. V. Kamat, and R. Ranjan, *Influence of Substrate Temperature on Structure, Microstructure and Magnetic Properties of Sputtered Fe-Ga Thin Films*, J. Magn. Magn. Mater. **384**, 58 (2015).

[60] L.-X. Ye, C.-M. Lee, J.-M. Lee, W.-L. Tseng, and T. Wu, *The Effect of Electrode and Annealing on CoFeB-MgO-TbFeCo*, IEEE Trans. Magn. **48**, 2820 (2012).

[61] A. Talapatra, J. Arout Chelvane, and J. Mohanty, *Tuning Magnetic Microstructure in Gd-Fe Thin Films: Experiment and Simulation*, J. Magn. Magn. Mater. **448**, 360 (2018).

[62] C.-M. Lee, L.-X. Ye, J.-M. Lee, T.-H. Hsieh, J. Syu, W. Chen, C. Huang, and T. Wu, *Magnetic Properties of Ultrathin TbFeCo Magnetic Films With Perpendicular Magnetic Anisotropy*, IEE **45**, 4023 (2009).

[63] J. Sato, Y. Murakami, H. Fuji, K. Kojima, A. Takahashi, R. Nakatani, and M. Yamamoto, *Pinning Effect Induced by Underlayer in TbFeCo Magnetic Recording Media*, Jpn. J. Appl. Phys. **47**, 150 (2008).

[64] H. Katayama, K. Watanabe, K. Takayama, J. I. Sato, S. Miyanishi, K. Kojima, and K. Ohta, *Effect of Underlayers of Laser-Assisted Magnetic Recording Media on High-Density Recording*, Appl. Phys. Lett. **81**, 4994 (2002).

[65] L. X. Ye, R. C. Bhatt, C. M. Lee, W. H. Hsu, and T. ho Wu, *Perpendicular Magnetic Anisotropy in TbFeCo/MgO Structure with Ta- and Hf-Underlayer*, J. Magn. Magn. Mater. **502**, 166554 (2020).

[66] S. Q. Yin, X. Q. Li, X. G. Xu, J. Miao, and Y. Jiang, *Effect of Ta Underlayer on Perpendicular Anisotropy of TbFeCo Films*, IEEE Trans. Magn. **47**, 3129 (2011).

[67] K. Vahaplar, A. M. Kalashnikova, A. V. Kimel, D. Hinzke, U. Nowak, R.

Chantrell, A. Tsukamoto, A. Itoh, A. Kirilyuk, and T. Rasing, *Ultrafast Path for Optical Magnetization Reversal via a Strongly Nonequilibrium State*, Phys. Rev. Lett. **103**, 117201 (2009).

[68] D. Popova, A. Bringer, and S. Blügel, *Theory of the Inverse Faraday Effect in View of Ultrafast Magnetization Experiments*, Phys. Rev. B - Condens. Matter Mater. Phys. **84**, 1 (2011).

[69] J. Hohlfeld, T. Gerrits, M. Bilderbeek, T. Rasing, H. Awano, and N. Ohta, *Fast Magnetization Reversal of GdFeCo Induced by Femtosecond Laser Pulses*, Phys. Rev. B - Condens. Matter Mater. Phys. **65**, 012413 (2002).

[70] D. Guarisco, R. Burgermeister, C. Stamm, and F. Meier, *Magnetization Reversal in the Picosecond Range Measured with Time-Resolved Magneto-Optical Kerr Effect*, Appl. Phys. Lett. **68**, 1729 (1996).

[71] M. Aeschlimann, A. Vaterlaus, M. Lutz, M. Stampanoni, F. Meier, H. C. Siegmann, S. Klahn, and P. Hansen, *High-Speed Magnetization Reversal near the Compensation Temperature of Amorphous GdTbFe*, Appl. Phys. Lett. **59**, 2189 (1991).

[72] C. D. Stanciu, A. Tsukamoto, A. V. Kimel, F. Hansteen, A. Kirilyuk, A. Itoh, and T. Rasing, *Subpicosecond Magnetization Reversal across Ferrimagnetic Compensation Points*, Phys. Rev. Lett. **99**, 217207 (2007).

[73] C. D. Stanciu, F. Hansteen, A. V. Kimel, A. Kirilyuk, A. Tsukamoto, A. Itoh, and T. Rasing, *All-Optical Magnetic Recording with Circularly Polarized Light*, Phys. Rev. Lett. **99**, 1 (2007).

[74] D. Steil, S. Alebrand, A. Hassdenteufel, M. Cinchetti, and M. Aeschlimann, *All-Optical Magnetization Recording by Tailoring Optical Excitation Parameters*, Phys. Rev. B - Condens. Matter Mater. Phys. **84**, 224408 (2011).

[75] R. K. Basumatary, Aakansha, B. Basumatary, B. Brahma, R. Hussain, S. Ravi, R. Brahma, and S. K. Srivastava, *Magnetic Property of CoTbNi Ternary Alloy Thin Films*, J. Supercond. Nov. Magn. **33**, 3165 (2020).

[76] R. Hussain, Aakansha, S. Ravi, and S. K. Srivastava, *Influence of Substrate (Si and Glass), Cu under-Layer, in Situ Annealing of Ta/Cu and Post-Annealing on Magnetic Properties of [Co(0.3 Nm)/Ni(0.6 Nm)]$_{4,10}$ Multilayer Thin Films*,

J. Mater. Sci. Mater. Electron. **31**, 11975 (2020).

[77] R. Hussain, Aakansha, B. Brahma, R. K. Basumatary, R. Brahma, S. Ravi, and S. K. Srivastava, *Sperimagnetism in Perpendicularly Magnetized Co-Tb Alloy-Based Thin Films*, J. Supercond. Nov. Magn. **32**, 4027 (2019).

[78] S. K. Srivastava, R. Hussain, T. Hauet, and L. Piraux, *Magnetization Reversal and Switching Field Distribution in Co-Tb Based Bit Patterned Media*, AIP Conf. Proc. **2115**, 1 (2019).

[79] T. Hauet et al., *Reversal Mechanism, Switching Field Distribution, and Dipolar Frustrations in Co/Pt Bit Pattern Media Based on Auto-Assembled Anodic Alumina Hexagonal Nanobump Arrays*, Phys. Rev. B - Condens. Matter Mater. Phys. **89**, 1 (2014).

[80] R. Hussain, Aakansha, S. Ravi, and S. K. Srivastava, *Magnetic Properties of Ordered Array of Nanobumps of [Co/Ni]$_{4,10,20}$ Multilayers*, Solid State Commun. **324**, 114144 (2021).

[81] L. Piraux, V. A. Antohe, F. Abreu Araujo, S. K. Srivastava, M. Hehn, D. Lacour, S. Mangin, and T. Hauet, *Periodic Arrays of Magnetic Nanostructures by Depositing Co/Pt Multilayers on the Barrier Layer of Ordered Anodic Alumina Templates*, Appl. Phys. Lett. **101**, (2012).

[82] J. C. A. Huang, Y. C. Chang, C. C. Yu, Y. D. Yao, Y. M. Hu, and C. M. Fu, *Mn Doping Effect on Structure and Magnetism of Epitaxial (FePt)1-XMnx Films*, J. Appl. Phys. **93**, 8173 (2003).

[83] P. Lu and S. H. Charap, *High Density Magnetic Recording Media Design and Identification : Susceptibility to Thermal Decay*, **31**, 2767 (1995).

[84] Y. B. Li, Y. F. Lou, L. R. Zhang, B. Ma, J. M. Bai, and F. L. Wei, *Effect of Magnetic Field Annealing on Microstructure and Magnetic Properties of FePt Films*, J. Magn. Magn. Mater. **322**, 3789 (2010).

[85] B. Yao and K. R. Coffey, *Quantification of L10 Phase Volume Fraction in Annealed [Fe/Pt]n Multilayer Films*, J. Appl. Phys. **105**, 0 (2009).

[86] J. Park, Y. K. Hong, S. G. Kim, L. Gao, and J. U. Thiele, *Magnetic Properties of Fe-Mn-Pt for Heat Assisted Magnetic Recording Applications*, J. Appl. Phys.

117, 3 (2015).

[87] Y. F. Ding, J. S. Chen, and E. Liu, *Structural and Magnetic Properties of FePt Films Grown on $Cr_{1-x}Mo_x$ Underlayers*, Appl. Phys. A Mater. Sci. Process. **81**, 1485 (2005).

[88] D. Weller, O. Mosendz, G. Parker, S. Pisana, and T. S. Santos, *$L1_0$ FePtX-Y Media for Heat-Assisted Magnetic Recording*, Phys. Status Solidi A **210**, 1245 (2013).

[89] R. Sbiaa, H. Meng, and S. N. Piramanayagam, *Materials with Perpendicular Magnetic Anisotropy for Magnetic Random Access Memory*, Phys. Status Solidi - Rapid Res. Lett. **5**, 413 (2011).

[90] J. M. Slaughter, *Materials for Magnetoresistive Random Access Memory*, Annu. Rev. Mater. Res. **39**, 277 (2009).

[91] Y. N. Hsu, S. Jeong, D. E. Laughlin, and D. N. Lambeth, *Effects of Ag Underlayers on the Microstructure and Magnetic Properties of Epitaxial FePt Thin Films*, J. Appl. Phys. **89**, 7068 (2001).

[92] S. C. Chen, P. C. Kuo, C. Y. Chou, and A. C. Sun, *Effects of Ag Buffer Layer on the Microstructure and Magnetic Properties of Nanocomposite FePt/Ag Multilayer Films*, J. Appl. Phys. **97**, 10 (2005).

[93] Y. F. Ding, X. Zhao, and E. Liu, *L10 FePt (001) Thin Films for Perpendicular Magnetic Recording Media*, in *Magnetic Thin Films: Properties, Performance and Applications*, edited by J. P. Volkerts (Nova Science Publishers, 2011), pp. 1–27.

[94] T. Mahalingam, J. P. Chu, J. H. Chen, C. L. Chiang, and S. F. Wang, *Synthesis and Characterization of $Fe_{100-x}Pt_x$ Alloy Thin Films*, Mater. Chem. Phys. **82**, 335 (2003).

[95] M. F. Toney, W. Y. Lee, J. A. Hedstrom, and A. Kellock, *Thickness and Growth Temperature Dependence of Structure and Magnetism in FePt Thin Films*, J. Appl. Phys. **93**, 9902 (2003).

[96] J. U. Thiele, L. Folks, M. F. Toney, and D. K. Weller, *Perpendicular Magnetic Anisotropy and Magnetic Domain Structure in Sputtered Epitaxial FePt (001)*

L10 Films, J. Appl. Phys. **84**, 5686 (1998).

[97] T. Suzuki, T. Kiya, N. Honda, and K. Ouchi, *High Density Recording on Ultra-Thin Fe-Pt Films of Perpendicular Composite Media*, IEEE Trans. Magn. **36**, 2417 (2000).

[98] T. Suzuki, H. Muraoka, Y. Nakamura, and K. Ouchi, *Design and Recording Properties of Fe-Pt Perpendicular Media*, IEEE Trans. Magn. **39**, 691 (2003).

[99] M. L. Yan, X. Z. Li, L. Gao, S. H. Liou, D. J. Sellmyer, R. J. M. Van De Veerdonk, and K. W. Wierman, *Fabrication of Nonepitaxially Grown Double-Layered FePt:C/FeCoNi Thin Films for Perpendicular Recording*, Appl. Phys. Lett. **83**, 3332 (2003).

[100] T. Suzuki and K. Ouchi, *Sputter-Deposited (Fe – Pt)– MgO Composite Films for Perpendicular Recording Media*, IEEE Trans. Magn. **37**, 1283 (2001).

[101] P. C. Kuo, S. C. Chen, Y. D. Yao, A. C. Sun, and C. C. Chiang, *Microstructure and Magnetic Properties of Nanocomposite FePtCr-SiN Thin Films*, J. Appl. Phys. **91**, 8638 (2002).

[102] B. M. Lairson, M. R. Visokay, R. Sinclair, and B. M. Clemens, *Epitaxial PtFe(001) Thin Films on MgO(001) with Perpendicular Magnetic Anisotropy*, Appl. Phys. Lett. **62**, 639 (1993).

[103] B. M. Lairson and B. M. Clemens, *Enhanced Magneto-Optic Kerr Rotation in Epitaxial PtFe(001) and PtCo(001) Thin Films*, Appl. Phys. Lett. **63**, 1438 (1993).

[104] B. M. Lairson, M. R. Visokay, E. E. Marinero, R. Sinclair, and B. M. Clemens, *Epitaxial Tetragonal PtCo (001) Thin Films with Perpendicular Magnetic Anisotropy*, J. Appl. Phys. **74**, 1922 (1993).

[105] T. Maeda, T. Kai, A. Kikitsu, T. Nagase, and J. I. Akiyama, *Reduction of Ordering Temperature of an FePt-Ordered Alloy by Addition of Cu*, Appl. Phys. Lett. **80**, 2147 (2002).

[106] S. R. Lee, S. Yang, Y. K. Kim, and J. G. Na, *Microstructural Evolution and Phase Transformation Characteristics of Zr-Doped FePt Films*, J. Appl. Phys. **91**, 6857 (2002).

[107] S. R. Lee, S. Yang, Y. K. Kim, and J. G. Na, *Rapid Ordering of Zr-Doped FePt Alloy Films*, Appl. Phys. Lett. **78**, 4001 (2001).

[108] C. P. Luo and D. J. Sellmyer, *Structural and Magnetic Properties of FePt:SiO2 Granular Thin Films*, Appl. Phys. Lett. **75**, 3162 (1999).

[109] Y. Z. Zhou, J. S. Chen, G. M. Chow, and J. P. Wang, *Structure and Magnetic Properties of In-Plane Oriented FePt - Ag Nanocomposites*, J. Appl. Phys. **93**, 7577 (2003).

[110] X. H. Xu, H. S. Wu, F. Wang, and X. L. Li, *Structure and Magnetic Properties of FePt and FePt/Ag Thin Films Deposited by Magnetron Sputtering*, Thin Solid Films **472**, 222 (2005).

[111] C. P. Luo, Z. S. Shan, and D. J. Sellmyer, *Magnetic Viscosity and Switching Volumes of Annealed Fe/Pt Multilayers*, J. Appl. Phys. **79**, 4899 (1996).

[112] K. R. Coffey, M. A. Parker, and J. K. Howard, *High Anisotropy $L1_0$ Thin Films for Longitudinal Recording*, IEEE Trans. Magn. **31**, 2737 (1995).

[113] J. P. Liu, C. P. Luo, Y. Liu, and D. J. Sellmyer, *High Energy Products in Rapidly Annealed Nanoscale Fe/Pt Multilayers*, Appl. Phys. Lett. **72**, 483 (1998).

[114] D. Weller, G. Parker, O. Mosendz, E. Champion, B. Stipe, X. Wang, T. Klemmer, G. Ju, and A. Ajan, *A HAMR Media Technology Roadmap to an Areal Density of 4 Tb/In^2*, IEEE Trans. Magn. **50**, (2014).

[115] H. Y. Wang, X. K. Ma, Y. J. He, S. Mitani, and M. Motokawa, *Enhancement in Ordering of FePt Films by Magnetic Field Annealing*, Appl. Phys. Lett. **85**, 2304 (2004).

[116] A. Asthana, Y. K. Takahashi, Y. Matsui, and K. Hono, *Effect of Base Pressure on the Structure and Magnetic Properties of FePt Thin Films*, J. Magn. Magn. Mater. **320**, 250 (2008).

[117] W. B. Mi, J. Jin, and H. L. Bai, *Effect of Mn Doping on the Magnetic Properties of the Post-Annealed $Fe_{48}Pt_{52}$-C Composite Films*, Phys. Status Solidi Appl. Mater. Sci. **208**, 2198 (2011).

[118] S. K. Chen, F. T. Yuan, G. S. Chen, and W. C. Chang, *Structural and Magnetic*

Properties of Fe-Pt-Nb Sputtered Films, Phys. B Condens. Matter **327**, 366 (2003).

[119] C. Feng, Q. Zhan, B. Li, J. Teng, M. Li, Y. Jiang, and G. Yu, *Magnetic Properties and Microstructure of FePt/Au Multilayers with High Perpendicular Magnetocrystalline Anisotropy*, Appl. Phys. Lett. **93**, 10 (2008).

[120] M. Maret, C. Brombacher, P. Matthes, D. Makarov, N. Boudet, and M. Albrecht, *Anomalous X-Ray Diffraction Measurements of Long-Range Order in (001)-Textured $L1_0$ FePtCu Thin Films*, Phys. Rev. B - Condens. Matter Mater. Phys. **86**, 1 (2012).

[121] R. Cuadrado, T. J. Klemmer, and R. W. Chantrell, *Magnetic Anisotropy of $Fe_{1-y}X_yPt$-$L1_0$ [X = Cr, Mn, Co, Ni, Cu] Bulk Alloys*, Appl. Phys. Lett. **105**, 0 (2014).

[122] T. Ono, H. Nakata, T. Moriya, N. Kikuchi, S. Okamoto, O. Kitakami, and T. Shimatsu, *Experimental Investigation of Off-Stoichiometry and 3d Transition Metal (Mn, Ni, Cu)-Substitution in Single-Crystalline FePt Thin Films*, AIP Adv. **6**, 6 (2016).

[123] B. Wang, K. Barmak, and T. J. Klemmer, *The A1 to $L1_0$ Transformation in FePt Films with Ternary Alloying Additions of Mg , V , Mn , and B*, J. Appl. Phys. **109**, 07B739 (2011).

[124] Y. K. Takahashi, M. Ohnuma, and K. Hono, *Low-Temperature Fabrication of High-Coercivity $L1_0$ Ordered FePt Magnetic Thin Films by Sputtering*, Jpn. J. Appl. Phys. **40**, L1367 (2001).

[125] Y. K. Takahashi, M. Ohnuma, and K. Hono, *Ordering Process of Sputtered FePt Films*, J. Appl. Phys. **93**, 7580 (2003).

[126] D. A. Gilbert, L. W. Wang, T. J. Klemmer, J. U. Thiele, C. H. Lai, and K. Liu, *Tuning Magnetic Anisotropy in (001) Oriented $L1_0$ $(Fe_{1-x}Cu_x)_{55}Pt_{45}$ Films*, Appl. Phys. Lett. **102**, 1 (2013).

[127] Y. K. Takahashi, M. Ohnuma, and K. Hono, *Effect of Cu on the Structure and Magnetic Properties of FePt Sputtered Film*, J. Magn. Magn. Mater. **246**, 259 (2002).

[128] B. H. Li, C. Feng, T. Yang, J. Teng, Z. H. Zhai, G. H. Yu, and F. W. Zhu, *Effect of Composition on $L1_0$ Ordering in FePt and FePtCu Thin Films*, J. Phys. D. Appl. Phys. **39**, 1018 (2006).

[129] M. L. Yan, Y. F. Xu, and D. J. Sellmyer, *Nanostructure and Magnetic Properties of Highly (001) Oriented $L1_0$ $(Fe_{49}Pt_{51})_{1-x}Cu_x$ Films*, J. Appl. Phys. **99**, 08G903 (2006).

[130] K. Hono, Y. K. Takahashi, G. Ju, J. U. Thiele, A. Ajan, X. M. Yang, R. Ruiz, and L. Wan, *Heat-Assisted Magnetic Recording Media Materials*, MRS Bull. **43**, 93 (2018).

[131] P. C. Kuo, Y. D. Yao, C. M. Kuo, and H. C. Wu, *Microstructure and Magnetic Properties of the $(FePt)_{100-x}Cr_x$ Thin Films*, J. Appl. Phys. **87**, 6146 (2000).

[132] Y. J. Chiu, G.-J. Chen, Y.-H. Shih, C.-L. Wang, and S.-R. Jian, *Cr Additive Effects on the Nanostructure, Magnetic Properties, and Ordering Kinetics of FePtCu Thin Films*, Surf. Coatings Technol. **350**, 913 (2018).

[133] J. P. Chu, T. Mahalingam, and S. F. Wang, *The Structure and Magnetic Properties of Sputtered FePtM (M = Ta, Cr) Thin Films*, J. Phys. Condens. Matter **16**, 561 (2004).

[134] T. Suzuki, H. Kanazawa, and S. Akimasa, *Magnetic and Structural Properties of Quaternary $(Fe–Co–Ni)_{50}Pt_{50}$ Alloy Thin Films*, IEEE Trans. Magn. **38**, 2794 (2002).

[135] N. Y. Schmidt, R. Mondal, A. Donges, J. Hintermayr, C. Luo, H. Ryll, F. Radu, L. Szunyogh, U. Nowak, and M. Albrecht, *$L1_0$-Ordered $(Fe_{100-x}Cr_x)Pt$ Thin Films: Phase Formation, Morphology, and Spin Structure*, Phys. Rev. B **102**, 1 (2020).

[136] M. E. Gruner and P. Entel, *Structural and Magnetic Properties of Ternary $Fe_{1-x}Mn_xPt$ Nanoalloys from First Principles*, Beilstein J. Nanotechnol. **2**, 162 (2011).

[137] T. Burkert, O. Eriksson, S. I. Simak, A. V. Ruban, B. Sanyal, L. Nordström, and J. M. Wills, *Magnetic Anisotropy of L 10 FePt and $Fe_{1-x}Mn_x$ Pt*, Phys. Rev. B - Condens. Matter Mater. Phys. **71**, 1 (2005).

[138] E. A. Manoharan, G. Mankey, and Y. K. Hong, *Tuning the Magnetic Properties of $Fe_{50-x}Mn_xPt_{50}$ Thin Films*, J. Magn. Magn. Mater. **438**, 111 (2017).

[139] G. Meyer and J. U. Thiele, *Effective Electron-Density Dependence of the Magnetocrystalline Anisotropy in Highly Chemically Ordered Pseudobinary $(Fe_{1-x}Mn_x)_{50}Pt_{50}$ $L1_0$ Alloys*, Phys. Rev. B - Condens. Matter Mater. Phys. **73**, 1 (2006).

[140] B. Wang and K. Barmak, *Re-Evaluation of the Impact of Ternary Additions of Ni and Cu on the A1 to L10 Transformation in FePt Films*, J. Appl. Phys. **109**, 123916 (2011).

[141] D. C. Berry and K. Barmak, *Effect of Alloy Composition on the Thermodynamic and Kinetic Parameters of the A1 to $L1_0$ Transformation in FePt , FeNiPt , and FeCuPt Films Effect of Alloy Composition on the Thermodynamic and Kinetic Parameters of the A 1 to L1 $_0$ Transformation in FePt*, J. Appl. Phys. **102**, 024912 (2007).

[142] D. C. Berry and K. Barmak, *Time-Temperature-Transformation Diagrams for the A1 to $L1_0$ Phase Transformation in FePt and FeCuPt Thin Films*, J. Appl. Phys. **101**, 014905 (2007).

[143] J. U. Thiele, K. R. Coffey, M. F. Toney, J. A. Hedstrom, and A. J. Kellock, *Temperature Dependent Magnetic Properties of Highly Chemically Ordered $Fe_{55-x}Ni_xPt_{45}$ $L1_0$ Films*, J. Appl. Phys. **91**, 6595 (2002).

[144] D. Kaifeng, C. Xiaomin, Y. A. N. Junbing, C. Weiming, L. I. Peng, and Y. Xiaofei, *Effect of Ni Doping on the Microstructure and Magnetic Properties of FePt Films*, Rare Met. **28**, 257 (2009).

[145] M. L. Yan, Y. F. Xu, X. Z. Li, and D. J. Sellmyer, *Highly (001) -Oriented Ni-Doped L 1_0 FePt Films and Their Magnetic Properties*, J. Appl. Phys. **97**, 10H309 (2005).

[146] J. L. Tsai, J. C. Huang, and H. W. Tai, *Magnetic Properties and Microstructure of Perpendicular FePt(B-Ag) Granular Films*, J. Appl. Phys. **111**, 07A709 (2012).

[147] L. Zhang, L. Liu, W. Pei, H. Liu, D. Gao, Q. Lin, J. Xie, F. Xiong, and W. Hu, *Magnetic Properties and Structure of $L1_0$ FePtC Films Prepared by Using the*

Electric Treatment, J. Alloys Compd. **868**, 159087 (2021).

[148] D. B. Xu, C. J. Sun, J. S. Chen, S. M. Heald, B. Sanyal, R. A. Rosenberg, T. J. Zhou, and G. M. Chow, *Large Enhancement of Magnetic Moment in $L1_0$ Ordered FePt Thin Films by Nd Substitutional Doping*, J. Phys. D. Appl. Phys. **48**, (2015).

[149] C. Gang, G. Zhengfei, Z. Huaiying, C. Jun, and Y. Songliu, *Effects of Pr on the Structure and Magnetic Properties of FePt Alloys*, Rare Met. **26**, 19 (2007).

[150] N. Y. Schmidt, S. Abdulazhanov, J. Michalička, J. Hintermayr, O. Man, O. Caha, M. Urbánek, and M. Albrecht, *Effect of Gd Addition on the Structural and Magnetic Properties of $L1_0$-FePt Alloy Thin Films*, J. Appl. Phys. **132**, 213908 (2022).

[151] A. Obeidat, B. Al-Aderah, and M. K. Qaseer, *Influence of Oxygen and Nitrogen Doping on the Structure and Magnetic Properties of CoNi Alloy: First Principle Calculations*, J. Phys. Chem. Solids **218**, 111963 (2023).

[152] J. Chen, C. Sun, and G. M. Chow, *A Review of $L1_0$ FePt Films for High-Density Magnetic Recording*, Int. J. Prod. Dev. **5**, 238 (2008).

[153] Y. Hsu, S. Jeong, D. N. Lambeth, and D. E. Laughlin, *In Situ Ordering of FePt Thin Films by Using Ag/Si and Ag/Mn_3Si/Ag/Si Templates*, IEEE Trans. Magn. **36**, 2945 (2000).

[154] P. V. Makushko, M. N. Shamis, N. Y. Schmidt, I. E. Kotenko, S. Gulyas, G. L. Katona, T. I. Verbytska, D. L. Beke, M. Albrecht, and I. M. Makogon, *Formation of Ordered $L1_0$-FePt Phase in FePt–Ag Thin Films*, Appl. Nanosci. **10**, 4809 (2020).

[155] Y. Xu, J. S. Chen, and J. P. Wang, *In Situ Ordering of FePt Thin Films with Face-Centered-Tetragonal (001) Texture on $Cr_{100-x}Ru_x$ Underlayer at Low Substrate Temperature*, Appl. Phys. Lett. **80**, 3325 (2002).

[156] J. S. Chen, Y. Xu, and J. P. Wang, *Effect of Pt Buffer Layer on Structural and Magnetic Properties of FePt Thin Films*, J. Appl. Phys. **93**, 1661 (2003).

[157] J. S. Chen, B. C. Lim, Y. F. Ding, and G. M. Chow, *Low-Temperature Deposition of $L1_0$ FePt Films for Ultra-High Density Magnetic Recording*, J.

Magn. Magn. Mater. **303**, 309 (2006).

[158] Y. Zhu and J. W. Cai, *Low-Temperature Ordering of FePt Thin Films by a Thin AuCu Underlayer*, Appl. Phys. Lett. **87**, 032504 (2005).

[159] P. Chaudhari, J. J. Cuomo, and R. J. Gambino, *Amorphous Metallic Films for Magneto-Optic Applications*, Appl. Phys. Lett. **22**, 337 (1973).

[160] D. W. Forester, C. Vittoria, J. Schelleng, and P. Lubitz, *Magnetostriction of Amorphous TbxFe1-x Thin Films*, J. Appl. Phys. **49**, 1966 (1978).

[161] Y. Hayashi, T. Honda, K. I. Arai, K. Ishiyama, and M. Yamaguchi, *Dependence of Magnetostriction of Sputtered Tb-Fe Films on Preparation Conditions*, IEEE Trans. Magn. **29**, 3129 (1993).

[162] H. Xu, C. Jiang, X. Jiang, and S. Gong, *Magnetic Anisotropy in (Tb0. 3Dy0.7)45Fe55 Amorphous Films*, J. Magn. Magn. Mater. **232**, 46 (2001).

[163] H. A. M. Van Den Berg, W. Clemens, G. Gieres, G. Rupp, W. Schelter, and M. Vieth, *GMR Sensor Scheme with Artificial Antiferromagnetic Subsystem*, IEEE Trans. Magn. **32**, 4624 (1996).

[164] J. Amaral, V. Pinto, T. Costa, J. Gaspar, R. Ferreira, E. Paz, S. Cardoso, and P. P. Freitas, *Integration of TMR Sensors in Silicon Microneedles for Magnetic Measurements of Neurons*, IEEE Trans. Magn. **49**, 3512 (2013).

[165] C. Bellouard, B. George, G. Marchal, N. Maloufi, and J. Eugène, *Influence of the Thickness of the CoFe Layer on the Negative Spin-Valve Effect in CoFe/Ag/CoFeGd Trilayers*, J. Magn. Magn. Mater. **165**, 312 (1997).

[166] X. J. Bai, J. Du, J. Zhang, B. You, L. Sun, W. Zhang, A. Hu, and S. M. Zhou, *Influence of the Thickness of the FeCoGd Layer on the Magnetoresistance in FeCoGd-Based Spin Valves and Magnetic Tunnel Junctions*, J. Phys. D. Appl. Phys. **41**, (2008).

[167] X. Jiang, L. Gao, J. Z. Sun, and S. S. P. Parkin, *Temperature Dependence of Current-Induced Magnetization Switching in Spin Valves with a Ferrimagnetic CoGd Free Layer*, Phys. Rev. Lett. **97**, 1 (2006).

[168] A. V. Svalov, G. V. Kurlyandskaya, and V. O. Vas'kovskiy, *Thermo-Sensitive Spin Valve Based on Layered Artificial Ferrimagnet*, Appl. Phys. Lett. **108**, 1

(2016).

[169] M. Milyaev, L. Naumova, T. Chernyshova, V. Proglyado, I. Kamensky, T. Krinitsina, M. Ryabukhina, and V. Ustinov, *Magnetization Reversal and Inverted Magnetoresistance of Exchange-Biased Spin Valves with a Gadolinium Layer*, J. Appl. Phys. **121**, (2017).

[170] F. Radu, R. Abrudan, I. Radu, D. Schmitz, and H. Zabel, *Perpendicular Exchange Bias in Ferrimagnetic Spin Valves*, Nat. Commun. **3**, 1 (2012).

[171] W. Zhang, D. Zhang, P. K. J. Wong, H. Yuan, S. Jiang, G. Van Der Laan, Y. Zhai, and Z. Lu, *Selective Tuning of Gilbert Damping in Spin-Valve Trilayer by Insertion of Rare-Earth Nanolayers*, ACS Appl. Mater. Interfaces **7**, 17070 (2015).

[172] R. Mishra, J. Yu, X. Qiu, M. Motapothula, T. Venkatesan, and H. Yang, *Anomalous Current-Induced Spin Torques in Ferrimagnets near Compensation*, Phys. Rev. Lett. **118**, 1 (2017).

[173] N. Roschewsky, T. Matsumura, S. Cheema, F. Hellman, T. Kato, S. Iwata, and S. Salahuddin, *Spin-Orbit Torques in Ferrimagnetic GdFeCo Alloys*, Appl. Phys. Lett. **109**, 112403 (2016).

[174] N. Roschewsky, C. H. Lambert, and S. Salahuddin, *Spin-Orbit Torque Switching of Ultralarge-Thickness Ferrimagnetic GdFeCo*, Phys. Rev. B **96**, 064406 (2017).

[175] D. Bang, P. Van Thach, and H. Awano, *Current-Induced Domain Wall Motion in Antiferromagnetically Coupled Structures: Fundamentals and Applications*, J. Sci. Adv. Mater. Devices **3**, 389 (2018).

[176] S. S. P. Parkin, M. Hayashi, and L. Thomas, *Magnetic Domain-Wall Racetrack Memory*, Science (80-.). **320**, 190 (2008).

[177] S. H. Yang, K. S. Ryu, and S. Parkin, *Domain-Wall Velocities of up to 750 Ms-1 Driven by Exchange-Coupling Torque in Synthetic Antiferromagnets*, Nat. Nanotechnol. **10**, 221 (2015).

[178] A. Hassdenteufel, C. Schubert, B. Hebler, H. Schultheiss, J. Fassbender, M. Albrecht, and R. Bratschitsch, *All-Optical Helicity Dependent Magnetic*

Switching in Tb-Fe Thin Films with a MHz Laser Oscillator, Opt. Express **22**, 10017 (2014).

[179] A. Ciuciulkaite et al., *Magnetic and All-Optical Switching Properties of Amorphous Tb_xCo_{100-x} Alloys*, Phys. Rev. Mater. **4**, 1 (2020).

[180] S. Alebrand, U. Bierbrauer, M. Hehn, M. Gottwald, O. Schmitt, D. Steil, E. E. Fullerton, S. Mangin, M. Cinchetti, and M. Aeschlimann, *Subpicosecond Magnetization Dynamics in TbCo Alloys*, Phys. Rev. B **89**, 1 (2014).

[181] S. Alebrand, M. Gottwald, M. Hehn, D. Steil, M. Cinchetti, D. Lacour, E. E. Fullerton, M. Aeschlimann, and S. Mangin, *Light-Induced Magnetization Reversal of High-Anisotropy TbCo Alloy Films*, Appl. Phys. Lett. **101**, 1 (2012).

[182] C. H. Back, R. Allenspach, W. Weber, S. S. P. Parkin, D. Weller, E. L. Garwin, and H. C. Siegmann, *Minimum Field Strength in Precessional Magnetization Reversal*, Sience **285**, 864 (1999).

[183] S. Kaka and S. E. Russek, *Precessional Switching of Submicrometer Spin Valves*, Appl. Phys. Lett. **80**, 2958 (2002).

[184] Y. F. Ding, J. S. Chen, E. Liu, C. J. Sun, and G. M. Chow, *Effect of Lattice Mismatch on Chemical Ordering of Epitaxial L1 0 FePt Films*, J. Appl. Phys. **97**, 10H303 (2005).

[185] K. Sin, J. M. Sivertsen, and J. H. Judy, *Surface Roughness and Magnetic Properties of in Situ Heated and Postannealed Thin Films of Perpendicular Barium Ferrite*, J. Appl. Phys. **75**, 5972 (1994).

[186] T. Seki, S. Mitani, K. Yakushiji, and K. Takanashi, *Spin-Polarized Current-Induced Magnetization Reversal in Perpendicularly Magnetized L10-FePt Layers*, Appl. Phys. Lett. **88**, 172504 (2006).

[187] G. Giannopoulos, L. Reichel, A. Markou, I. Panagiotopoulos, V. Psycharis, C. Damm, S. Fähler, I. Khan, J. Hong, and D. Niarchos, *Optimization of L10 FePt/$Fe_{45}Co_{55}$ Thin Films for Rare Earth Free Permanent Magnet Applications*, J. Appl. Phys. **117**, 223909 (2015).

[188] P. J. Kelly and R. D. Arnell, *Magnetron Sputtering: A Review of Recent*

Developments and Applications, Vacuum **56**, 159 (2000).

[189] D. Depla, S. Mahieu, and J. E. Greene, *Sputter Deposition Process*, in *Handbook of Deposition Technologies for Films and Coatings*, Third Edit, Vol. 281 (Elsevier, 2010), pp. 253–296.

[190] M. Barun, *Magnetron Sputterin Technique*, https://doi.org/10.1007/978-1-4471-4670-4_28.

[191] A. Anders, *Plasma and Ion Sources in Large Area Coating: A Review*, Surf. Coatings Technol. **200**, 1893 (2005).

[192] W. R. Grove, *VII. On the Electro-Chemical Polarity of Gases*, Philos. Trans. R. Soc. London **142**, 87 (1852).

[193] ., https://www.filmetrics.com/profilometers/profilm3d.

[194] M. Marrese, V. Guarino, and L. Ambrosio, *Atomic Force Microscopy: A Powerful Tool to Address Scaffold Design in Tissue Engineering*, J. Funct. Biomater. **8**, 1 (2017).

[195] S. Chatterjee, S. S. Gadad, and T. K. Kundu, *Atomic Force Microscopy*, Resonance.

[196] F. J. Giessibl, *Advances in Atomic Force Microscopy*, Rev. Mod. Phys. **75**, 949 (2003).

[197] R. García and R. Pérez, *Dynamic Atomic Force Microscopy Methods*, Surf. Sci. Rep. **47**, 197 (2002).

[198] H. Ris and M. Malecki, *High-Resolution Field Emission Scanning Electron Microscope Imaging of Internal Cell Structures after Epon Extraction from Sections: A New Approach to Correlative Ultrastructural and Immunocytochemical Studies*, J. Struct. Biol. **111**, 148 (1993).

[199] D.-S. Yang, O. F. Mohammed, and A. H. Zewail, *Scanning Ultrafast Electron Microscopy*, Phys. Sci. **107**, 14993 (2014).

[200] H. Chang, S. M. Iqbal, E. A. Stach, A. H. King, N. J. Zaluzec, and R. Bashir, *Fabrication and Characterization of Solid-State Nanopores Using a Field Emission Scanning Electron Microscope*, Appl. Phys. Lett. **88**, 103109 (2006).

[201] B. D. Culity and S. R. Stock, *Elements of X-Ray Diffraction*, Third (Pearson,

Harlow, 2014).

[202] M. Zakaullah, K. Alamgir, M. Shafiq, S. M. Hassan, M. Sharif, and A. Waheed, *Enhanced Copper K-Alpha Radiation from a Low-Energy Plasma Focus*, Appl. Phys. Lett. **78**, 877 (2001).

[203] S. Foner, *Versatile and Sensitive Vibrating Sample Magnetometer*, Rev. Sci. Instrum. **30**, 548 (1959).

[204] S. Foner, *The Vibrating Sample Magnetometer: Experiences of a Volunteer (Invited)*, J. Appl. Phys. **79**, 4740 (1996).

[205] S. Foner, *Further Improvements in Vibrating Sample Magnetometer Sensitivity*, Rev. Sci. Instrum. **46**, 1425 (1975).

[206] S. Foner, *Vibrating Sample Magnetometer*, Rev. Sci. Instrum. **27**, 548 (1956).

[207] I. Galili, D. Kaplan, and Y. Lehavi, *Teaching Faraday's Law of Electromagnetic Induction in an Introductory Physics Course*, Am. J. Phys. **74**, 337 (2006).

[208] R. Kingman, S. C. Rowland, and S. Popescu, *An Experimental Observation of Faraday's Law of Induction*, Am. J. Phys. **70**, 595 (2002).

[209] C. L. Fleck, Magnetism in the Complex Cobaltates Y1−xSrxCoO3−δ (0.7 ≤ x ≤ 0.95) and $Ca_3Co_2O_6$, University of Warwick, 2011.

[210] S. Tumanski, *H A N D B O O K O F MAGNETIC MEASUREMENTS*, First (CRC Press; Taylor & Francis Group, Boca, Raton, 2011).

[211] R. K. Basumatary, P. Behera, B. Basumatary, B. Brahma, S. Ravi, R. Brahma, and S. K. Srivastava, *Influence of Surface Roughness on Magnetic Properties of CoTbNi Ternary Alloy Films*, Micro and Nanostructures **174**, 207491 (2023).

[212] F. Rafieian, M. Mousavi, A. Dufresne, and Q. Yu, *Polyethersulfone Membrane Embedded with Amine Functionalized Microcrystalline Cellulose*, Int. J. Biol. Macromol. **164**, 4444 (2020).

[213] Z. B. Fang, Z. J. Yan, Y. S. Tan, X. Q. Liu, and Y. Y. Wang, *Influence of Post-Annealing Treatment on the Structure Properties of ZnO Films*, Appl. Surf. Sci. **241**, 303 (2005).

[214] A. Z. Simões, A. H. M. González, M. A. Zaghete, J. A. Varela, and B. D.

Stojanovic, *Effects of Annealing on the Crystallization and Roughness of PLZT Thin Films*, Thin Solid Films **384**, 132 (2001).

[215] C. C. Chang, X. D. Wu, R. Ramesh, X. X. Xi, T. S. Ravi, T. Venkatesan, D. M. Hwang, R. E. Muenchausen, S. Foltyn, and N. S. Nogar, *Origin of Surface Roughness for C-Axis Oriented Y-Ba-Cu-O Superconducting Films*, Appl. Phys. Lett. **57**, 1814 (1990).

[216] J. P. B. Silva, K. C. Sekhar, A. Almeida, J. A. Moreira, M. Pereira, and M. J. M. Gomes, *Influence of Laser Repetition Rate on Ferroelectric Properties of Pulsed Laser Deposited $BaTiO_3$ Films on Platinized Silicon Substrate*, Appl. Phys. A Mater. Sci. Process. **113**, 379 (2013).

[217] K. Wang, Y. Huang, Z. Xu, S. Dong, and R. Chen, *Effect of Sputtering Power on the Magnetic Properties of Amorphous Perpendicular TbFeCo Films*, J. Magn. Magn. Mater. **424**, 89 (2017).

[218] C. T. Lie, P. C. Kuo, C. Y. Chou, S. C. Chen, T. H. Wu, and A. C. Sun, *Microstructure and Magnetic Properties of $Co_{70.5-x}Tb_{29.5}Pd_x$ Films*, J. Magn. Magn. Mater. **272**–**276**, 353 (2004).

[219] M. Yanagisawa, *Magnetic Properties and Structures of Sputtered CoNi/Cr Films*, IEEE Trans. Magn. **MAG**-**22**, 576 (1986).

[220] E. Aubry, T. Liu, A. Billard, A. Dekens, F. Perry, S. Mangin, and T. Hauet, *Influence of the Cr and Ni Concentration in CoCr and CoNi Alloys on the Structural and Magnetic Properties*, J. Magn. Magn. Mater. **422**, 391 (2017).

[221] C. Papusoi, A. Stancu, and J. L. Dormann, *The Initial Susceptibility in the FC and ZFC Magnetisation Processes*, J. Magn. Magn. Mater. **174**, 236 (1997).

[222] G. Aravind, M. Raghasudha, and D. Ravinder, *Synthesis, Characterization and FC-ZFC Magnetization Studies of Cobalt Substituted Lithium Nano Ferrites*, J. Magn. Magn. Mater. **378**, 278 (2015).

[223] M. F. Hansen and S. M, *Estimation of Blocking Temperatures from ZFC / FC Curves*, J. Magn. Magn. Mater. **203**, 214 (1999).

[224] P. Hansen, *Hand Book of Magnetic Materials* (North-Holland, Amsterdam, 1991).

[225] J. M. D. Coey, *Materials, Magnetism and Magnetic*, 1st ed. (CAMBRIDGE UNIVERSITY PRESS, Newyork, 2009).

[226] K. Ueda, A. J. Tan, and G. S. D. Beach, *Effect of Annealing on Magnetic Properties in Ferrimagnetic GdCo Alloy Films with Bulk Perpendicular Magnetic Anisotropy*, AIP Adv. **8**, (2018).

[227] R. C. Taylor and A. Gangulee, *Magnetization and Magnetic Anisotropy in Evaporated GdCo Amorphous Films*, J. Appl. Phys. **47**, 4666 (1976).

[228] V. G. Harris, K. D. Aylesworth, B. N. Das, W. T. Elam, and N. C. Koon, *Structural Origins of Magnetic Anisotropy in Amorphous Fe-Tb Films and Multilayers*, Phys. Rev. Lett. **69**, 1939 (1992).

[229] and F. H. V. G. Harris, W. T. Elam, N. C. Koon, *Deposition-Temperature Dependence of Structural Anisotropy in Amorphous Tb-Fe Films*, Phys. Rev. B **49**, 3637 (1994).

[230] S.-C. N. Cheng, M. H. Kryder, and M. C. A. Mathur, *Stress Related Anisotropy Studies in DC-Magnetron Sputtered TbCo and TbFe Films*, IEEE Trans. Magn. **25**, 4018 (1989).

[231] and P. M. Hong Fu, Masud Mansuripur, *Generic Source of Perpendicular Anisotropy in Amorphous Rare-Earth-Transition-Metal Films*, Phys. Rev. Lett. **66**, 4 (1991).

[232] X. Yan, M. Hirscher, T. Egami, and E. E. Marinero, *Direct Observation of Anelastic Bond-Orientational Anisotropy in Amorphous* $Tb_{26}Fe_{62}Co_{12}$ *Thin Films by x-Ray Diffraction*, Phys. Rev. B **43**, 9300 (1991).

[233] A. T. Hindmarch, A. W. Rushforth, R. P. Campion, C. H. Marrows, and B. L. Gallagher, *Origin of In-Plane Uniaxial Magnetic Anisotropy in CoFeB Amorphous Ferromagnetic Thin Films*, Phys. Rev. B - Condens. Matter Mater. Phys. **83**, 1 (2011).

[234] Y. Mimura and N. Imamura, *Magnetic Properties of Amorphous Tb-Fe Thin Films Prepared by Rf Sputtering*, Appl. Phys. Lett. **28**, 746 (1976).

[235] R. K. Basumatary, H. Basumatary, M. M. Raja, R. Brahma, and S. K. Srivastava, *Tuning Magnetic Properties of FePtCo Ternary Alloy Thin Films*

for Magnetic Storage Device Application, J. Alloys Compd. **955**, 170313 (2023).

[236] T. Mahalingam, J. P. Chu, J. H. Chen, S. F. Wang, and K. Inoue, *Microstructure and Magnetic Properties of Sputtered Fe-Pt Thin Films*, J. Phys. Condens. Matter **15**, 2561 (2003).

[237] R. Dinnebier, *Rietveld Refinement from Powder Diffraction Data*, Vol. December 2 (2001).

[238] L. B. Mccusker, R. B. Von Dreele, D. E. Cox, D. Louër, and P. Scardi, *Rietveld Refinement Guidelines*, J. Appl. Crystallogr. **32**, 36 (1999).

[239] L. W. Finger, D. E. Cox, and A. P. Jephcoat, *A Correction for Powder Diffraction Peak Asymmetry Due to Axial Divergence BY*, J. Appl. Crystallogr. **27**, 892 (1994).

[240] R. Yogamalar, R. Srinivasan, A. Vinu, K. Ariga, and A. C. Bose, *X-Ray Peak Broadening Analysis in ZnO Nanoparticles*, Solid State Commun. **149**, 1919 (2009).

[241] S. Mustapha, M. M. Ndamitso, A. S. Abdulkareem, J. O. Tijani, D. T. Shuaib, A. K. Mohammed, and A. Sumaila, *Comparative Study of Crystallite Size Using Williamson-Hall and Debye-Scherrer Plots for ZnO Nanoparticles*, Adv. Nat. Sci. Nanosci. Nanotechnol. **10**, (2019).

[242] U. Holzwarth and N. Gibson, *The Scherrer Equation versus the "Debye-Scherrer Equation,"* Nat. Nanotechnol. **6**, 534 (2011).

[243] D. B. Xu, C. J. Sun, J. S. Chen, S.-W. Han, S. M. Heald, R. A. Rosenberg, and G. M. Chow, *Investigation of Spin and Orbital Moments of $L1_0$ FePtRh Thin Films*, J. Appl. Phys. **111**, 07C120 (2012).

List of Papers Published in Journals and Conferences

Sections of the work described in this thesis have been published in the following journal articles

1. **R. K. Basumatary**, Aakansha, B. Basumatary, B. Brahma, R. Hussain, S. Ravi, R. Brahma and S. K. Srivastava, "*Magnetic Property of CoTbNi Ternary Alloy Thin Films*", Journal of Superconductivity and Novel Magnetism, **33**, 3165–3170 (2020)

2. **R. K. Basumatary**, P. Behera, B. Basumatary, B. Brahma, S. Ravi, R. Brahma, S.K. Srivastava, "*Influence of surface roughness on magnetic properties of CoTbNi ternary alloy films*" Micro and Nanostructures, **174**, 207491 (2023)

3. **R. K. Basumatary**, H. Basumatary, M. M. Raja, R. Brahma and S. K. Srivastava, "*Tuning of Magnetic Properties of FePtCo Ternary Alloy Thin Films for Magnetic Storage Device Application*", Journal of Alloys and Compounds **955**, 170313 (2023)
4. **R. K. Basumatary,** R. Brahma and S. K. Srivastava, "Influence of film surface roughness on magnetic properties of sputter deposited FePtCo alloy films. (*submitted*)

Section of the work has been submitted for publication as book chapter

1. **R. K. Basumatary**, R. Brahma, S. K. Srivastava, "*Surface Topography and Surface Roughness Study of CoTbNi Alloy Thin Films using 3D Optical Profilometer".* (Submitted in PANE-2022)

The work described in this thesis has also been presented in talks and posters at the following conferences

1. **R. K. Basumatary**, Aakansha, S. Ravi, R. Brahma and S. K. Srivastava, "*Fabrication, Surface Roughness and Magnetic Property of Nanoscale* $(Co_{0.85}Tb_{0.15})_{0.46}Ni_{0.54}$ *Alloy Thin Film*", International Conference on Advanced Nanomaterials and Nanotechnology (ICANN) (18-21 December 2019), IIT Guwahati (Poster presentation)

2. **R. K. Basumatary**, S. Ravi, R. Brahma and S. K. Srivastava, *3D Surface Topography and Surface Roughness measurement of CoTb based RE-TM ternary*

Alloy Thin Films using Optical Imaging Technique, National Conference on Advances in Sustainable Chemistry and Material Science (ASCMS), (29-30 April 2022), Bodoland University (Oral presentation)

3. **R. K. Basumatary**, R. Brahma, S. K. Srivastava, "*Surface Topography and Surface Roughness Study of CoTbNi Alloy Thin Films using 3D Optical Profilometer*", National Conference of Physics Academy of North East (PANE), (8-10 November 2022), Manipur University (Poster presentation)

Publications

Journal of Alloys and Compounds 955 (2023) 170313

Contents lists available at ScienceDirect

Journal of Alloys and Compounds

journal homepage: www.elsevier.com/locate/jalcom

Tuning magnetic properties of FePtCo ternary alloy thin films for magnetic storage device application

R.K. Basumatary [a,c], H. Basumatary [b], M.M. Raja [b], R. Brahma [c,*], S.K. Srivastava [d,*]

[a] Department of Physics, Darrang College, Tezpur, Assam 784001, India
[b] Defence Metallurgical Research Laboratory, Kanchanbagh, Hyderabad 500058, India
[c] Department of Physics, Bodoland University, Kokrajhar, Assam 783370, India
[d] Department of Physics, CIT Kokrajhar, Kokrajhar, Assam 783370, India

A R T I C L E I N F O

Article history:
Received 1 February 2023
Received in revised form 14 April 2023
Accepted 25 April 2023
Available online 26 April 2023

Keywords:
FePtCo thin films
Magnetic anisotropy
Effective anisotropy constant
Magnetron sputtering
Annealing
Cu-underlayer

A B S T R A C T

FePtCo ternary alloy films have been grown on Si-substrate by co-sputtering of Co with FePt under three conditions i.e., as-deposited, in-situ annealed, and with Cu-underlayer using a DC magnetron sputtering. The film surface roughness, crystal structure, and magnetic properties of these films were investigated. The average surface roughness (S_a and R_a) of these films deposited under three deposition conditions slightly varies in the range of 0.41–2.48 nm with the increase of Co content. The XRD results show that all the films crystallize in a close-packed FCC structure. The lattice parameters and average crystallite size decrease with an increase in Co concentration for all deposited conditions. The magnetic measurement indicates that the as-deposited films exhibit low coercivity and excellent in-plane magnetic anisotropy with a large effective anisotropy energy in the range of $1.22 \times 10^6 - 1.88 \times 10^7$ erg/cc. The increase of Co content in as-deposited FePtCo films leads to a reduction in the saturation magnetization (M_S) and K_{eff} by promoting anti-ferromagnetic interaction with FePt sublattice. However, the annealing and insertion of a 2 nm Cu-underlayer further help to enhance the ferromagnetic nature and as a result, the value of M_S and K_{eff} is enhanced with an increase of Co content.

1. Introduction

Recently thin films of metallic multilayers and rare-earth transition metal alloys have drawn the considerable interest to the scientific community for their potential application in magnetic storage media [1–10]. For decades, $L1_0$ ordered FePt thin films have drawn the attention of researchers remarkably because of their potential applications in high density heat assisted magnetic recording (HAMR) media due to their large magnetic anisotropy energy density [11–14]. Under normal deposition condition, FePt films are usually grown in disordered FCC structure [15,16] which has low magnetic anisotropy energy density with easy axis along the film plane and possesses soft magnetic properties [12]. However, for application in perpendicular magnetic recording technology, the FePt film must be fully transformed from disordered FCC to $L1_0$ phase. The $L1_0$ ordered FCT structure can be achieved either by post-annealing of as-deposited films at temperatures above 450 °C [16–21] or by depositing the films at elevated substrate temperature (in-situ annealing) above 500°C [22–25]. It was observed that upon annealing of the films, the FCC changes to $L1_0$ ordered with easy axis tilted 35° away from the film plane, which can be further tuned in direction perpendicular to film plane [15,16]. Several investigations on FePt alloy films, FePt/Ag bilayer films, and FePtAg ternary alloy thin films have been reported due to their potential application to replace present conventional CoCrPt-based storage media [26,27]. For application in high areal density (~ Tb/in^2) recording media, FePt-based films should have high magnetocrystalline anisotropy energy, high saturation magnetization (M_S) and beyond room temperature Curie temperature [28]. The material properties like magnetic anisotropy, curie temperature, structural ordering temperature, and crystallographic orientation of FePt alloy film can be manipulated by adding third elements such as Au, Ag, Cr, Mn, Cu, Ni, etc. [13,22,26,29–33]. It was further reported that the base pressure of the deposition chamber also plays a significant role in lowering of ordering temperature of FePt alloy thin films [34]. Several theoretical studies have been performed based on first principle calculations on doping of third elements such as Mn to FePt by replacing Fe with [35,36]. However, their results showed that anisotropy constant and coercivity decrease with an increase in Mn content and also increased antiferromagnetic interaction. Doping of

* Corresponding authors.
E-mail addresses: rajibhcu@gmail.com (R. Brahma), sk.srivastava@cit.ac.in (S.K. Srivastava).

https://doi.org/10.1016/j.jallcom.2023.170313
0925-8388/

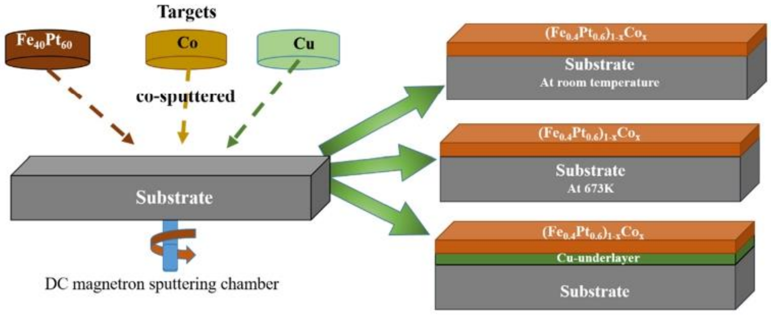

Fig. 1. Schematic diagram of sputtering deposition of FePtCo thin films using magnetron sputtering system.

rare-earth elements such as Nd, Tb, etc. as third elements has also been reported for applications of permanent magnet and sensor applications [22,37]. In the present report, we have attempted to study the structural and magnetic properties of FePtCo alloy thin films prepared by dc magnetron sputtering. We have studied the influence of addition of Co to FePt deposited under various deposition conditions such as; as-deposited, annealing at a temperature below which disordered FCC to $L1_0$ ordered FCT transition takes place, and insertion of Cu-underlayer on the magnetic properties of FePtCo thin fims. So, the main objective of present manuscript is to study the influence of Co addition on magnetic properties of FCC phase of FePtCo thin films prepared under various conditions in a correlation with crystal structure and surface roughness.

2. Experimental details

The $(Fe_{0.4}Pt_{0.6})_{1-x}Co_x$ (x = 0, 0.11, 0.17, 0.28 and 0.30) ternary alloy thin films have been grown on Si substrate (dimension 4 cm×2.5 cm) using a UHV magnetron sputtering (Make: LJ Equipment, Model: LJHUV SP5) system. The ternary alloy thin films were deposited by co-sputtering of pure Co target with $Fe_{40}Pt_{60}$ alloy target at 5 mTorr (base pressure) under Ar gas environment (as shown in Fig. 1). The three sets of samples were prepared under three different deposition conditions, first: deposited at room temperature (as-deposited), second: deposited at substrate temperature 673 K (in-situ annealed) which is well below the temperature at which FCC to $L1_0$ FCT phase transition takes place, and third: first nonmagnetic Cu layer of 2 nm was deposited on Si substrate at room temperature and then FePtCo films were deposited on Cu layer (Cu-under layered). In the first two set of samples, one thin film of $Fe_{40}Pt_{60}$ alloy without co-sputtering of Co and four FePt thin films by adding third element Co, a total of five samples were prepared, and in the third set of samples four FePtCo thin films were prepared by co-sputtering of Co with $Fe_{40}Pt_{60}$ alloy target. In all samples, $Fe_{40}Pt_{60}$ was sputtered at the same power 25 watt and the Co target was sputtered at four different powers 25, 50, 75, and 100 watt to obtain varying Co content in the films. The deposition time of each sample was so maintained to keep the thickness of all samples approximately the same (100 nm). The thickness of all prepared films was measured using 3D optical profilometer (Make: Filmetrics, USA, Model: 3D Profilm). For thickness measurement, the films were deposited on the partially masked substrate to create step height of the films. After deposition, masks were removed and the step height of the film was measured by profilometer. The deposited samples were cut into small pieces for different characterization. The film surface topography and surface roughness were also measured by this profilometer and atomic force microscopy (Make: Bruker, Model: Innova). The compositions of the deposited thin films were estimated by energy dispersive x-ray spectroscopy (EDX) (Make: JEOL JAPAN, Model: JSM 6390LV) equipped with scanning electron microscope. The EDX calibration was performed by using Cu grid as reference standard materials. Measurements were performed at 15–20 kV and electron beam was scanned on a 50 μm × 70μm area during analysis. The structural property of the thin films was analyzed by Grazing incidence x-ray diffraction (GIXRD) machine (Make: Rigaku Corporation Japan, Model: Smart LAb) operated at 5.4 kW. The $\theta - 2\theta$ x-ray diffraction measurement was carried out using Co-Kα at room temperature and the data were collected after subtracting the substrate contribution. The magnetic properties were measured by vibrating sample magnetometer (VSM) (Make: MicroSense VSM USA, Model: EZ16) at room temperature in the applied magnetic field range of 0 to ±18000 Oe.

3. Results

The composition of the deposited thin films in relative atomic percentage was estimated by EDX spectroscopy. A representative

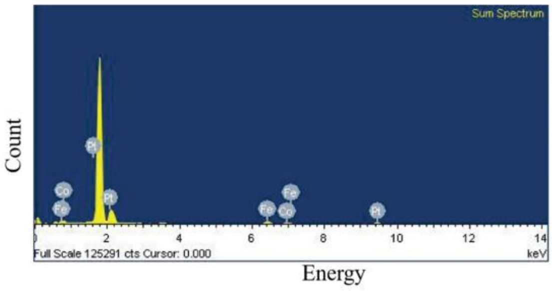

Element	Weight%	Atomic%
Fe K	13.98	31.85
Co K	7.98	17.23
Pt M	78.05	50.92
Totals	100.00	

Fig. 2. EDX spectrum (left) of $(Fe_{0.4}Pt_{0.6})_{1-x}Co_x$ film for which the Co target was sputtered at 50 watt. The right panel indicates the measured relative weight and atomic percentage of elements present in the sample. The exact composition has been found as $(Fe_{0.4}Pt_{0.6})_{0.83}Co_{0.17}$ i.e. with x = 0.17 (17 at% Co).

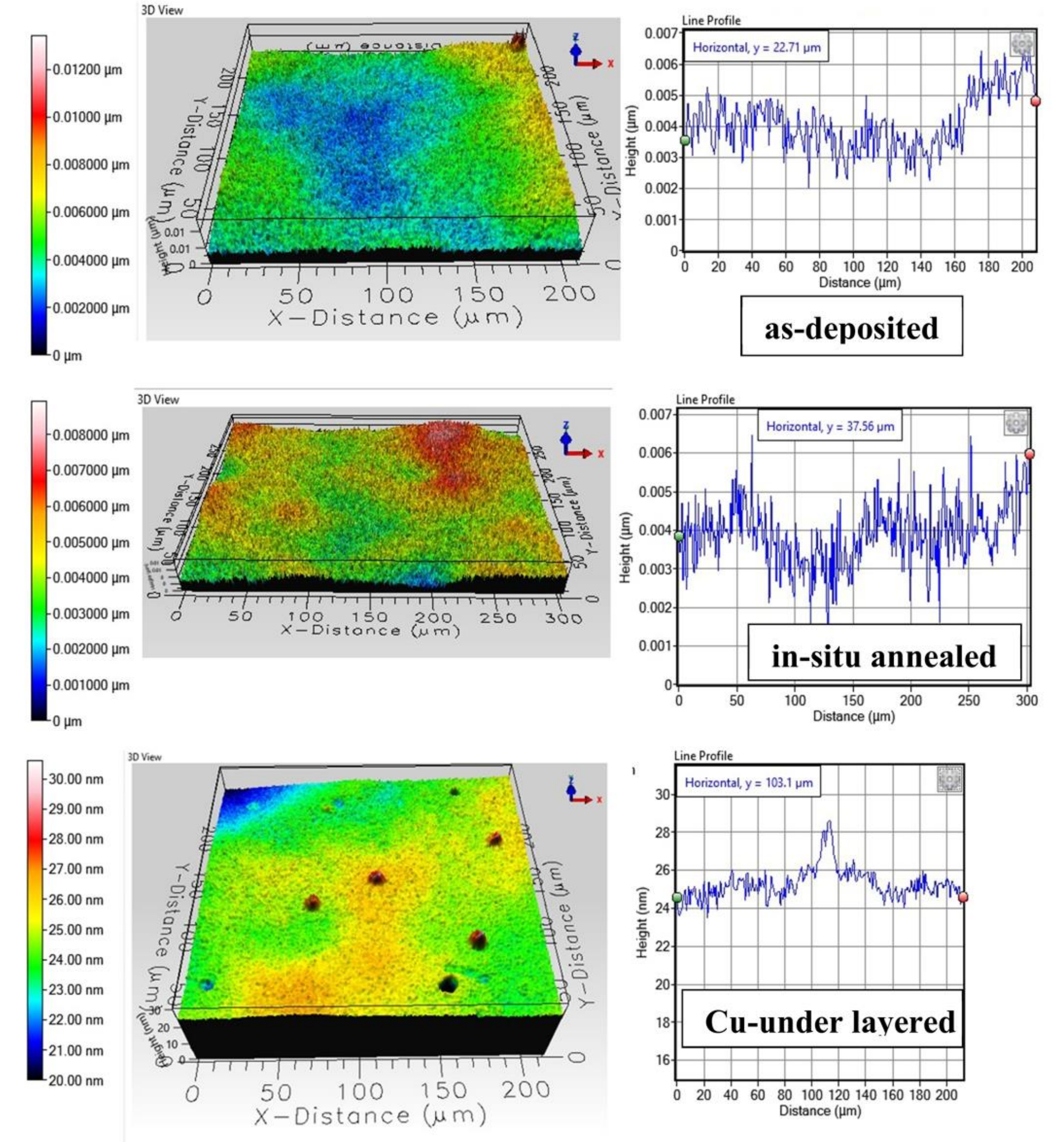

Fig. 3. 3D image of surface profile (middle) and line profile (right) with colour contrast z-scale (left) of $(Fe_{0.4}Pt_{0.6})_{0.89}Co_{0.11}$ ternary alloy thin films prepared under three deposition conditions.

EDX spectrum of as-deposited thin film of $(Fe_{0.4}Pt_{0.6})_{1-x}Co_x$ with Co target deposited at 50 watt has been presented in Fig. 2 for which the exact composition has been found as $(Fe_{0.4}Pt_{0.6})_{0.83}Co_{0.17}$ i.e. with x = 0.17 (17 at% Co). The obtained composition of the as-deposited thin films are found to be x = 0.11, 0.17, 0.28, and 0.30 for the films deposited with Co target power of 25, 50, 75, and 100 watt respectively. The Co content of the films are seen to increase with an increase in sputtering power as expected.

The thin film thickness and surface roughness were measured by 3D optical profilometer. To measure the thickness, the films were deposited on the partially masked substrate to create the step height of the film. After deposition, the masking tapes were removed and the step heights were measured using the step height mode of Profilm 3D optical profilometer. The thickness of the films was found to be approximately 100 nm for all deposited films. The average surface roughness S_a which is the average absolute distance of the

Table 1
S_a, R_a, lattice parameters, average crystallite size and room temperature magnetic parameters M_S, H_C, K_{eff} of as-deposited and in-situ annealed FePtCo alloy thin films. The quantity in the brackets indicate the error.

Sample	$(Fe_{0.4}Pt_{0.6})_{1-x}Co_x$		x = 0	x = 0.11	x = 0.17	x = 0.28	x = 0.30
As-deposited	S_a (nm)		1.41	1.11	0.81	0.76	2.48
	R_a (nm)		0.53	0.47	0.48	0.52	0.66
	R_a (nm) (AFM)		0.41	0.53	0.69	0.47	1.57
	Lattice parameters (Å)		3.821 (0.001)	3.804 (0.010)	3.799 (0.001)	3.762 (0.001)	3.746 (0.001)
	Fitting parameter (χ^2)		1.40	1.29	1.23	1.38	1.24
	Crystallite size (nm)		21.43	15.71	10.85	13.08	13.05
	M_S (emu/cc)		2036	1633	1691	1428	1155
	H_C (Oe)	In-plane	46	63	53	78	72
		Out-of-plane	177	237	91	82	31
	K_{eff} (erg/cc)		1.88×10^7	9.42×10^6	7.05×10^6	7.30×10^6	6.55×10^6
In-situ annealed	S_a (nm)		1.02	0.83	0.91	0.76	1.06
	R_a (nm)		0.53	0.54	0.48	0.52	0.52
	R_a (nm) (AFM)		0.23	0.44	0.40	-	-
	Lattice parameters (Å)		3.819 (0.001)	3.802 (0.005)	3.90 (0.002)	3.758 (0.001)	3.742 (0.005)
	Fitting parameter (χ^2)		1.69	1.20	1.18	1.94	1.29
	Crystallite size (nm)		14.44	17.71	-	11.57	9.88
	M_S (emu/cc)		2484	1780	471	1196	1283
	H_C (Oe)	In-plane	82	72	86	73	65
		Out-of-plane	14	931	33	47	200
	K_{eff} (erg/cc)		1.27×10^7	7.58×10^6	1.22×10^6	7.12×10^6	7.54×10^6

surface points from the mean plane [38] was measured in ISO 25178 height standard mode. The R_a; which is the average deviation of the roughness profile within the scanned length of the sample [39], was measured in ISO 4287 amplitude standard mode. The representative 3D images of the surface and line profile along with colour contrast z-scale of the film with Co 11 at% prepared under three deposition conditions are presented in Fig. 3 and the obtained values of S_a and R_a are listed in Table 1 and Table 2. The value of R_a varies along the different lines of measurement within the scanned area of the sample. So for the best result, the R_a is measured along the middle of the scanned area of the sample. The value of S_a of films ranges from 0.76 nm to 2.48 nm and R_a from 0.41 nm to 0.66 nm against the thickness of 100 nm of the films. The value of S_a of as-deposited films first slightly decreases with an increase of Co-content up to 17 at% and then increases with further increase in the Co-content of the film and it is plotted in later section as Fig. 8 (a). On the other hand, all compositions of annealed films have nearly the same values of S_a and R_a. These values of S_a and R_a are smaller than the S_a and R_a obtained for as-deposited films. This indicates that annealing of films reduces the film surface roughness which may be due to the migration of atoms during annealing. The Cu-under layered films have nearly the same S_a and R_a as that of annealed films except for x = 0.28 samples. The film surface roughness R_a is also measured using AFM. The representative 2D and 3D AFM images of 11 at% Co-doped $(Fe_{0.4}Pt_{0.6})_{0.89}Co_{0.11}$ film prepared under as-deposited, in-situ annealed and Cu-under layered are presented in Fig. 4. The obtained R_a of as-deposited and annealed films are presented in Table 1, and Cu-under layered films in Table 2. The R_a obtained from AFM measurement slightly differs from the R_a obtained from 3D optical profilometer and shows a small overall increase in the range of 0.23–1.57 nm with the increase in Co-doping. These results indicate that all films are relatively smooth for the films with thickness of 100 nm.

For structural analysis, x-ray diffraction (XRD) measurement was carried out for all samples at room temperature using Co-Kα radiation. The obtained XRD results show that all thin films prepared under three different conditions exhibit the face-centered cubic (FCC) structure with space group $Fm\bar{3}m$ No. 225. The results show that the in-situ annealing of films and insertion of Cu-underlayer (2 nm) do not affect the FCC phase of FePtCo alloy films. The results also reveal that the annealing temperature of 673 K is not sufficient for the formation of $L1_0$ FCT phase. To determine the lattice parameters, Rietveld refinement of the XRD pattern was carried out using FullProf Suite software [40–42]. The Rietveld refinement fit of XRD profiles of as-deposited, in-situ annealed, and Cu-under layered FePtCo thin films are presented in Figs. 5, 6 and Fig. 7 respectively and the obtained lattice parameters along with fitting parameters are presented in Table 1 and Table 2. From the XRD patterns, it is noticed that the annealing and insertion of Cu underlayer promote the (200) and (220) plane also. The lattice parameters of all FePtCo thin films deposited under the three conditions are found to vary with the film composition as depicted in Fig. 8(b). With an increase in Co content, the lattice parameters of as-deposited films show a systematic decrease from 3.822 Å for pure FePt to 3.746 Å for Co

Table 2
S_a, R_a, lattice parameters, average crystallite size and room temperature magnetic parameters M_S, H_C, K_{eff} of Cu under layered FePtCo alloy thin films. The quantity in the brackets indicate the error.

Sample	$(Fe_{0.4}Pt_{0.6})_{1-x}Co_x$		x = 0.11	x = 0.17	x = 0.28	x = 0.30
Cu-under layered	S_a (nm)		0.84	0.76	1.25	1.03
	R_a (nm)		0.41	0.41	0.54	0.44
	R_a (nm) (AFM)		0.507	0.365	0.928	0.915
	Lattice parameters (Å)		3.796 (0.001)	3.772 (0.001)	3.765 (0.001)	3.752 (0.001)
	Fitting parameter (χ^2)		1.48	1.53	1.35	1.83
	Crystallite size (nm)		18.01	11.22	10.27	11.86
	M_S (emu/cc)		2266	1010	1637	1482
	H_C (Oe)	In-plane	73	86	73	70
		Out-of-plane	132	276	118	225
	K_{eff} (erg/cc)		1.31×10^7	2.49×10^6	9.17×10^6	8.13×10^6

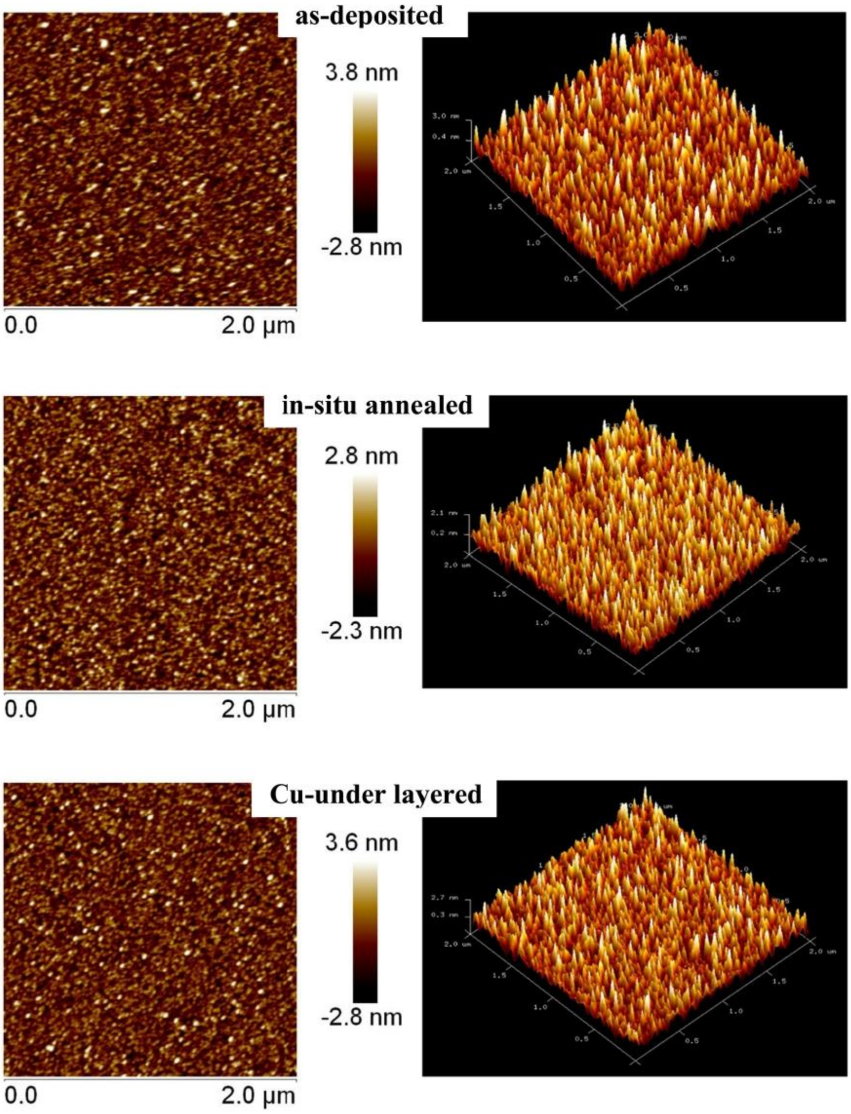

Fig. 4. 2D and 3D Atomic Force Microscopy images along with colour contrast scale of $(Fe_{0.4}Pt_{0.6})_{0.89}Co_{0.11}$ thin films prepared under three deposition conditions.

30 at% film and; for Cu-under layered films, it decreases from 3.796 Å for Co 11 at% to 3.752 Å for Co 30 at%. However, the in-situ annealed Co 17 at% film has the largest lattice parameters of 3.900 Å as can be seen in Fig. 8(b). For other in-situ annealed films lattice parameters decrease from 3.819 Å to 3.742 Å with increase in Co content. This is expected due to the smaller atomic radii of the Co atom (1.52 Å) [43] than the Pt atom (1.77 Å) [43] and hence the overall result indicate a decrease in the lattice parameters. Except 17 at% Co, all other films deposited under different conditions possess nearly the same lattice parameters and vary in a similar nature with Co addition. A dispersion of lattice parameters is observed for 17 at. Co doped films (see Fig. 8(b)), the largest being 3.900 Å for in-situ annealed and the least being 3.772 Å for Cu-under layered film. The peak position of the highest intensity XRD peak (111) and FWHM are obtained by fitting the XRD peak using the pseudo-voigt peak function and the average crystallite size of the films is calculated using Scherrer equation [44–46].

$$D_v = \frac{k\lambda}{\beta \cos\theta}$$

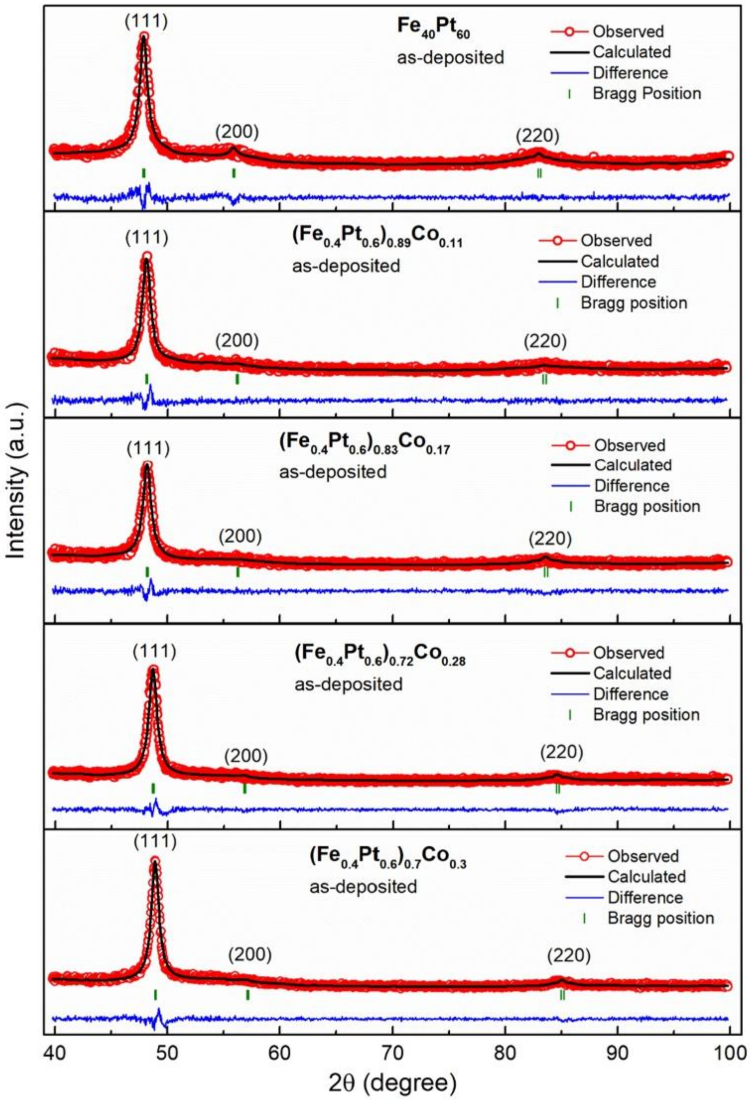

Fig. 5. XRD patterns along with the Rietveld refinement fitting of as-deposited FePtCo ternary alloy thin films.

Where λ(=1.79Å) is wavelength of the x-ray (Co-K_{α}), $k = 0.9$ is a constant, β is FWHM of XRD peak and θ is obtained by dividing peak position (2θ) by 2. Due to the large peak broadening of annealed Co 17 at% film, the peak could not be fitted and hence crystallite size could not be determined for this sample. The obtained average crystallite size of all prepared films is presented in Table 1 and Table 2. The variation of average crystallite size of all the samples has been plotted as a function of Co content of the samples and presented in Fig. 8(c). For the first three as-deposited samples up to Co 17 at%, reduction in crystallite size is observed from 21.43 nm to 10.85 nm. Above 17 at% it increases to 13.05 nm with further increase in Co addition. A similar variation in crystallite size is also observed for Cu-under layered films. On the other hand, in-situ annealing of films leads crystallite size to vary differently. The crystallite size first increases from 14.44 nm for pure FePt film to 17.71 nm Co 11 at%, thereafter decreases nearly linearly with further increase in the Co content of the films as depicted in Fig. 8(c). As the insertion of Cu underlayer and annealing of the films do not affect the FCC structure, it can be concluded that the dominant factor leading to variation of crystallite size with deposition conditions is the XRD peak broadening which may be due to the internal stresses of the crystal. Upon annealing and insertion of Cu underlayer, the intensity ratio of (111)

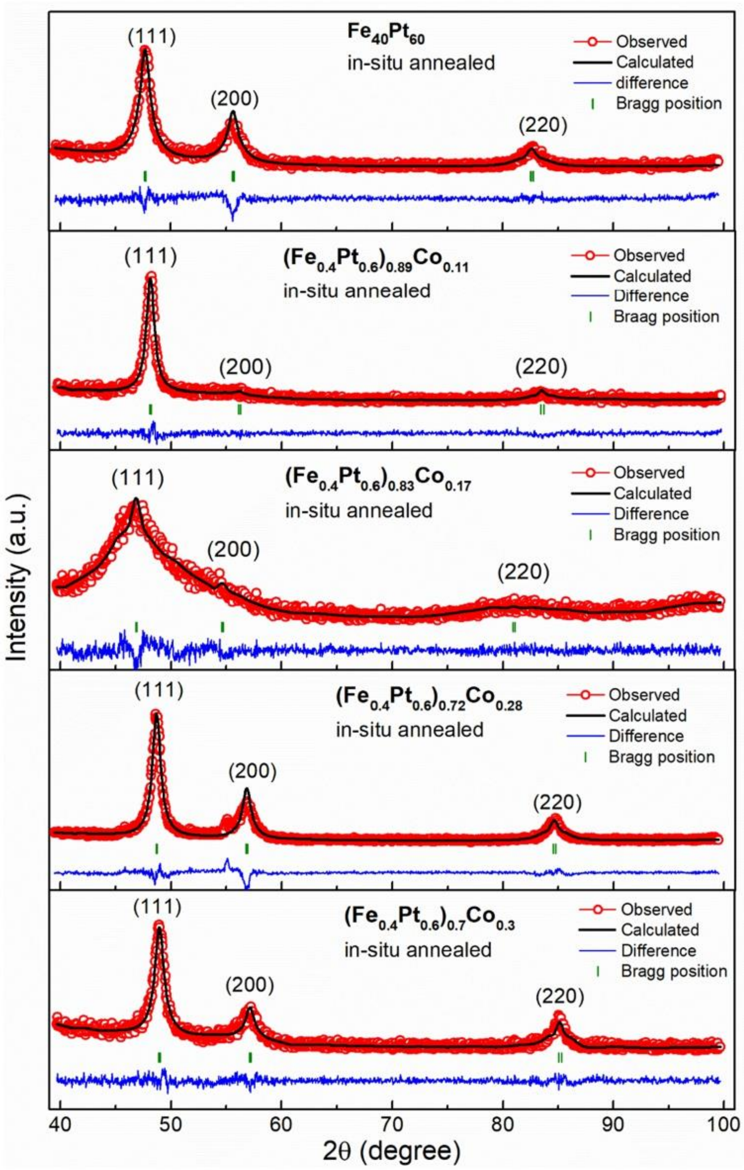

Fig. 6. XRD patterns along with the Rietveld refinement fitting of in-situ annealed FePtCo ternary alloy thin films at temperature 673 K.

peak to (200) and (220) peaks decreases. This suggests that annealing and insertion of Cu underlayer help pure FePt and Co-doped FePt films to grow in (200) and (220) directions.

The room temperature magnetization measurement as a function of applied field (M-H) of all the samples was carried out using VSM by applying field in two directions, one parallel to the plane of film (In-plane magnetization) and the other perpendicular to the plane of film (Out-of-plane magnetization). The measurement was carried out in the magnetic field range of 0 Oe to ±18000 Oe. The obtained M-H hysteresis loops and plot of the variation of coercive fields (H_C) and saturation magnetization (M_S) with film composition of as-deposited FePtCo thin films are presented in Fig. 9. All the in-plane magnetization of as-deposited thin films exhibits nearly square hysteresis loop. The coercive fields (H_C) of the in-plane magnetization are found to vary in a small range of 46–78 Oe with the increase in Co content of as-deposited thin films. On the other hand, the H_C of out-of-plane magnetization first increases from 177 Oe for $Fe_{0.4}Pt_{0.6}$ film to 273 Oe for Co 11 at%. With further increase in Co content, out-

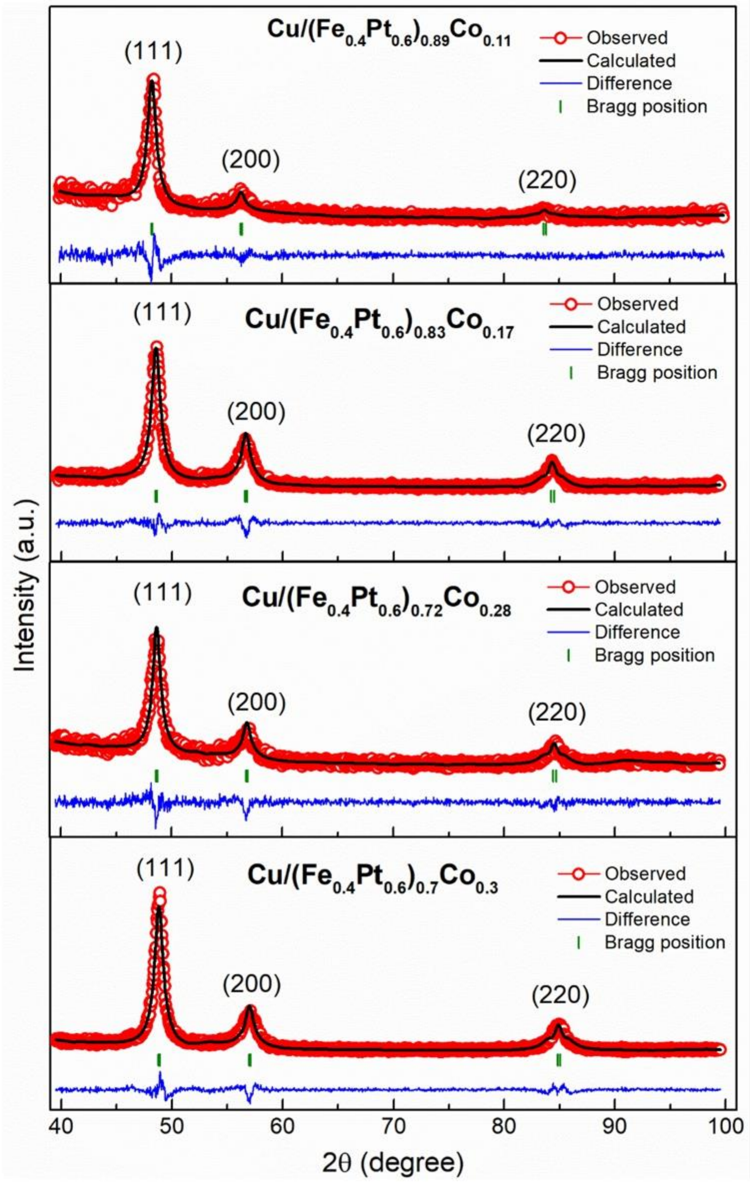

Fig. 7. XRD patterns along with Rietveld refinement fitting of FePtCo ternary alloy thin films deposited on Cu-underlayer.

of-plane H_C decreases to 31 Oe for 30 at% Co content film (Table 1). The values of out-of-plane H_C are greater than H_C of in-plane M-H loops indicating the films are magnetically harder in out-of-plane direction than in in-plane direction except for 30 at% Co-doped film. The saturation magnetization also shows a systematic decrease with an increase in Co content of the thin films from 2036 emu/cc for pure FePt film to 1155 emu/cc for the film with 30 at% Co (Table 1). It has also been observed that the in-plane magnetization of all as-deposited thin films saturate at a much lower field than the out-of-plane magnetization. This indicates that all as-deposited FePtCo thin films exhibit in-plane magnetic anisotropy with magnetic easy axis parallel to the film plane and magnetic hard axis perpendicular to the film plane. We have also estimated the effective anisotropy energy constant (K_{eff}) from M-H curves by calculating the area enclosed by in-plane and out-of-plane M-H curves. The difference in area enclosed by in-plane M-H curves and out-of-plane M-H curves

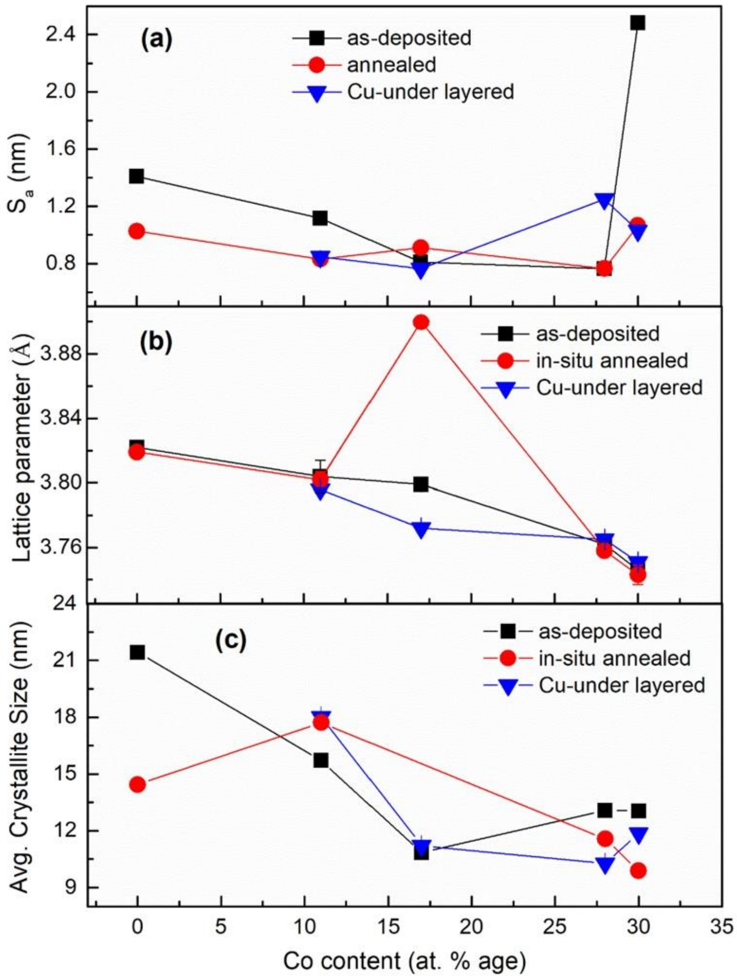

Fig. 8. Variation of (a) average surface roughness S_a, (b) lattice parameter and (c) average crystallite size as a function of Co content of FePtCo alloy thin films.

is the indicative effective anisotropic energy constant [1,30,47]. The obtained values of effective anisotropic energies are given in Table 1. Large values of K_{eff} are observed in all as-deposited thin films but the value of K_{eff} decreases from 1.88×10^7 erg/cc to 6.55×10^6 erg/cc with an increase in Co content from 0 to 30 at% as shown in Fig. 12 (b).

The room temperature M-H hysteresis curves of in-situ annealed thin films are presented in Fig. 10 and the obtained magnetic parameters are presented in Table 1. The in-plane H_C of annealed thin films shows a small variation with the film composition. However, the coercive field of out-of-plane M-H loops increases from 14 Oe to 200 Oe with the increase in Co-content of the films except for Co 11 at% film. The Co 11 at% film has an exceptionally large value of out-of-plane H_C 931 Oe. As can be seen from Table 1, the first three in-situ annealed thin films have larger values of in-plane H_C than the as-deposited films with the same composition, but for the last two samples with 28 and 30 at% Co, in-plane H_C is smaller than the corresponding as-deposited films. The most apparent impact of Co is on the saturation magnetization which strongly reduced from 2484 emu/cc to 471 emu/cc with the addition of Co up to 17 at%. With further increase in Co content above 17 at% nearly linear increase in M_S from 471 emu/cc to 1283 emu/cc is seen (bottom right corner of Fig. 10). The in-plane magnetization curves of all in-situ annealed FePtCo thin films saturate at a much smaller applied field than out-of-plane magnetization curves. This indicates that all in-situ annealed films also exhibit in-plane magnetic anisotropy with easy axis parallel to the film plane. The effective magnetic anisotropic constants are estimated from the area enclosed by in-plane and out-of-plane M-H curves and the obtained values of K_{eff} are presented in Table 1. The K_{eff} of annealed films is found to be smaller than the as-deposited films which suggests that annealing does not enhance magnetic anisotropy. Addition of Co up to 17 at% results reduction in K_{eff} from 1.27×10^7 erg/cc for pure FePt film to 1.22×10^6 erg/cc for Co 17 at%. Above 17 at%, Co addition results in a nearly linear increase in K_{eff} to 7.54×10^6 erg/cc for the film with

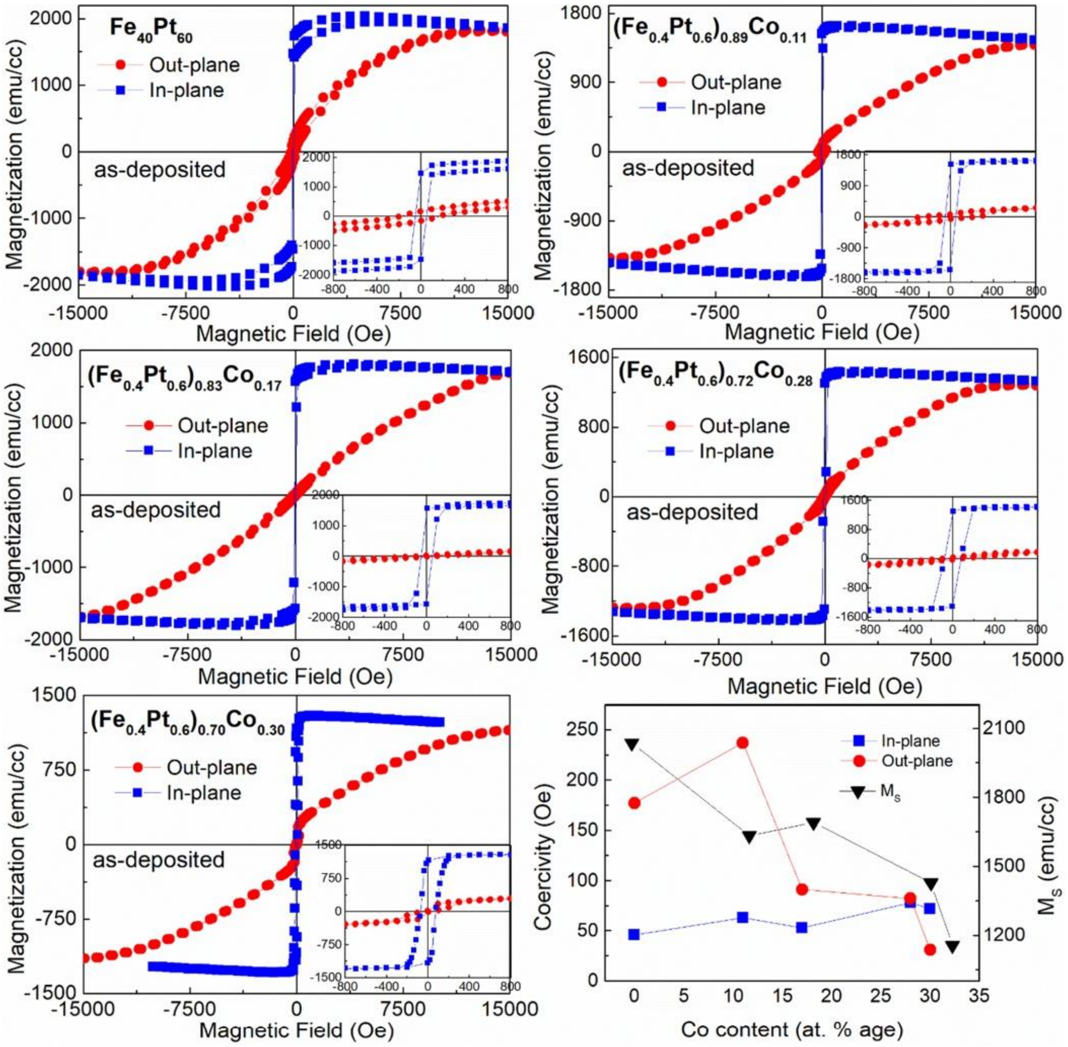

Fig. 9. Room temperature M-H hysteresis curves, and (bottom right corner) plot of variation of coercivity and saturation magnetization as a function of Co content of as-deposited FePtCo ternary alloy thin films.

30 at% Co. The nature of variation of K_{eff} is found to be similar to the variation of M_S with film compositions of these films as shown in Fig. 12 (b). This suggests that the Co-doping to FePt films promotes antiferromagnetic coupling up to 17 at% Co-doping as a result of which net magnetic moment decreases. With further increase in Co above 17 at%, ferromagnetic coupling again starts and the net magnetic magnetization starts increasing with an increase in Co addition. The room temperature M-H loops Cu under layered films also shows similar in-plane anisotropy behaviour to those of as-deposited and in-situ annealed films with easy axis parallel to film plane as shown in Fig. 11. The obtained M_S, H_C, and K_{eff} of Cu under layered films are presented in Table 1. The M_S of these films initially decreases with Co addition from 2266 emu/cc for 11 at% Co to 1010 emu/cc for film with Co 17 at% as can be seen in Fig. 12 (a). Above Co 17 at% M_S shows an overall increase with an increase in Co addition. The nature of variation M_S of Cu under layered films is similar to the variation of M_S of in-situ annealed films. However, the obtained values of M_S of Cu-under layered films are greater than the M_S of as-deposited and in-situ annealed thin films except for 17 at% Co film. This indicates that the insertion of Cu-underlayer enhances the net magnetization of FePtCo films. It also suggests that the addition of Co up to 17 at% favours antiferromagnetic interaction as a result of which a decrease in M_S is observed. With further increase in Co-doping beyond 17 at%, the magnetic interaction again changes to ferromagnetic as a result of which an appreciable increase in M_S has been observed in Cu-under layered films. The H_C of in-plane magnetization of these films is also found to vary slightly in the range of 70–86 Oe with film composition (Fig. 12 (a)). The effective magnetic anisotropic constants calculated from M-H curves of these films also show similar variation with film composition to in-situ annealed

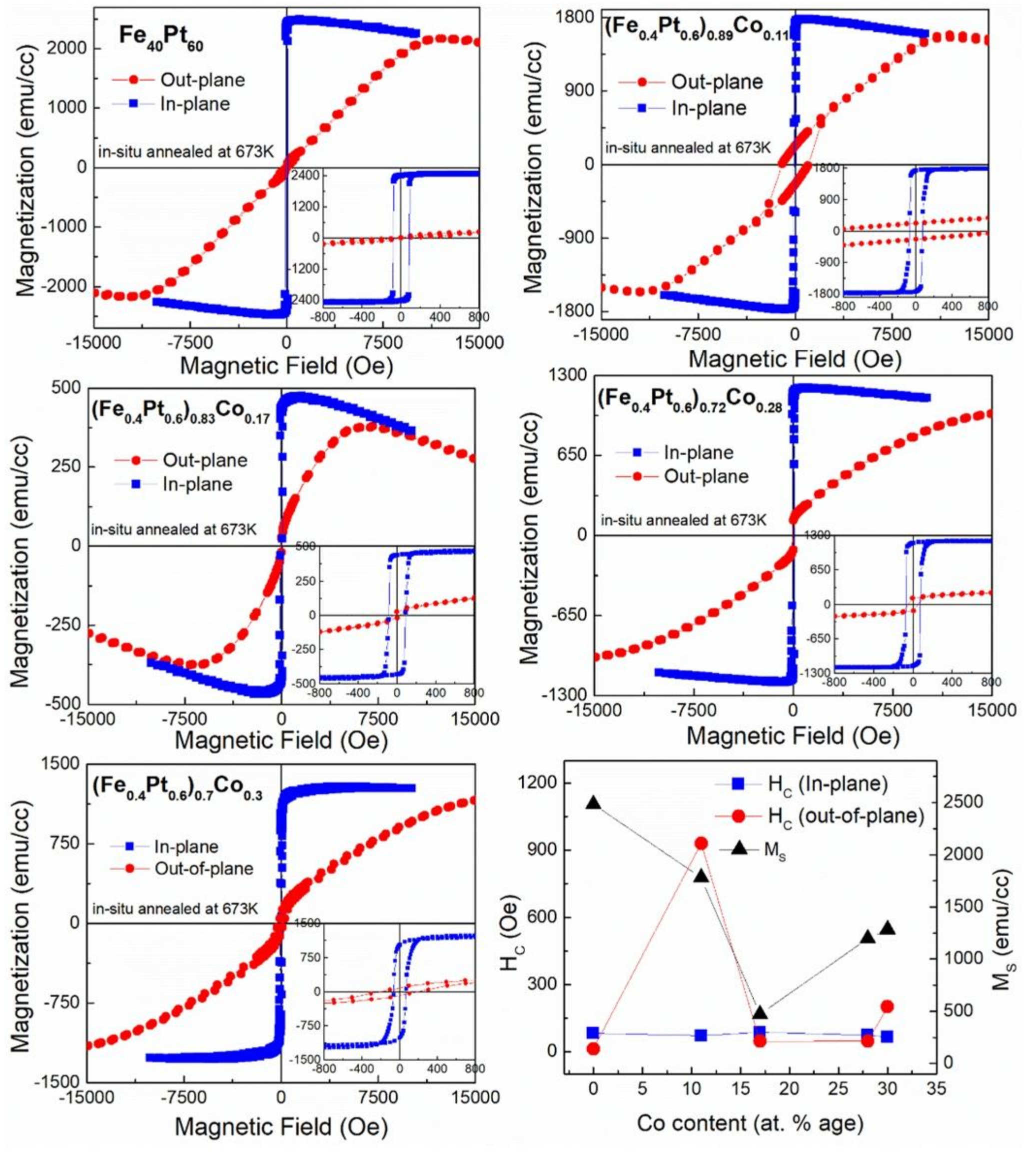

Fig. 10. Room temperature M-H hysteresis curves, and plot of variation of magnetic parameters H_C and M_S as a function of Co content of in-situ annealed FePtCo alloy thin films.

FePtCo films (see Fig. 12 (b)). The 17 at% Co-doped FePt film with Cu-underlayer has the least K_{eff} than other Cu-under layered films. With an increase or decrease in Co-doping the K_{eff} of the Cu-under layered films increases. All these observations suggest that K_{eff} is strongly film composition dependent irrespective of film deposition condition. The annealing of the films results in reduction in K_{eff} but the insertion of Cu-underlayer has improved the K_{eff} except for the film with 17 at% Co.

4. Discussion

Thus, the study of the film surface roughness, crystal structure, and magnetic properties of FePtCo ternary alloy films revealed many interesting features. The film surface roughness S_a and R_a of all films deposited under the three conditions measured using 3D optical profilometer as well as AFM varies in the range of 0.41–2.48 nm, which appears to be sufficiently smaller as compared to the thickness of

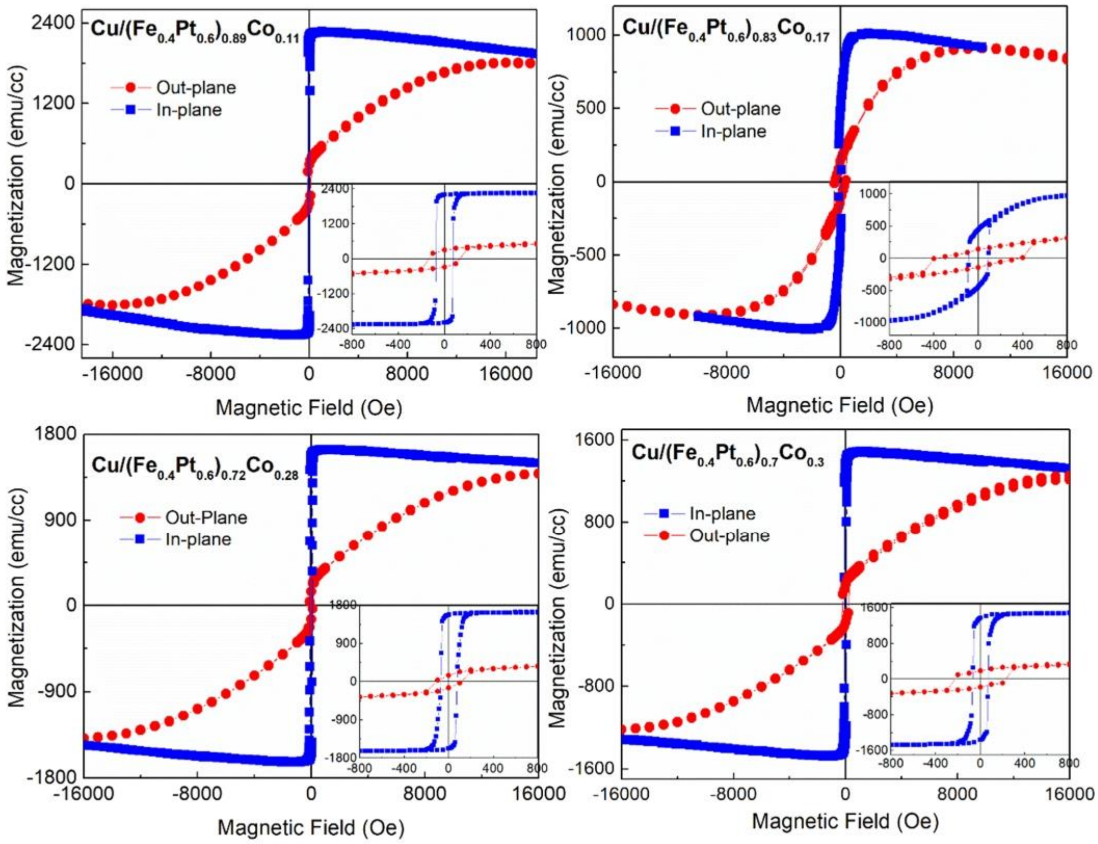

Fig. 11. Room temperature M-H hysteresis curves of FePtCo alloy thin films deposited on 2 nm Cu-underlayer.

100 nm of the films. These small film roughnesses are found insufficient to influence the magnetic property of these thin films. The FCC structure of as-deposited as well as Cu-under layered (2 nm) FePt thin films is not altered by the addition of third element Co up to 30 at% as observed in XRD patterns of these films. The annealing of the films at a temperature of 673 K is also seen as insufficient to transform the FCC structure of these films to $L1_0$ ordered structure. The most apparent impact of annealing and insertion of Cu underlayer on crystal structure is that they promote crystal growth in (200) and (220) directions along with (111) texture in contrast to as-deposition. Also the obtained magnetic parameters H_C, M_S and K_{eff} vary differently as compared to the variation in lattice parameters and average crystallite size. All these observations show that the magnetic properties of these films are solely controlled by Co content of FePtCo films. To emphasize the role of Co on the magnetic properties of FePtCo films, the saturation magnetization and effective magnetic anisotropic constant of as-deposited films are plotted as a function of Co content of the films in Fig. 13 and Fig. 12 respectively. For as-deposited thin films, the decrease in M_S with increase in Co content is attributed to the antiferromagnetic coupling of Co sublattice with FePt sublattice. Antiferromagnetic coupling of Co and FePt sublattice with unequal magnetic moment Co and FePt results in ferrimagnetic coupling. As a result of this, the net magnetization and effective anisotropic energy decrease with increase in Co content of as-deposited films. A similar observation has been reported in Mn-doped [24,35,36], and Nd-doped [37] FePt films. The annealing also enhances the net magnetization of pure FePt film, which decreases drastically with Co addition from 2484 emu/cc for pure FePt film to 471 emu/cc for Co 17 at% due to antiferromagnetic interaction between Co and FePt sublattice. On the other hand, the annealing results reduction in in-plane magnetic anisotropy as evident from Fig. 12 (b). The large difference in M_S and K_{eff} of as-deposited and in-situ annealed Co 17 at% film indicates the existence of a strong antiferromagnetic interaction at 17 at% Co. On further increase of Co addition to 30 at%, the Co promotes ferromagnetic coupling as a result of which M_S again starts increasing to 1283 emu/cc. A similar variation of K_{eff} of annealed FePtCo films is observed in Fig. 12 (b). This suggests that 17 at% is the optimum value of Co addition up to which antiferromagnetic coupling between Co and FePt dominates over ferromagnetic coupling and above which further Co addition favours ferromagnetic coupling. A Similar variation of magnetization and K_{eff} of Cu-under layered FePtCo films have been observed similar to annealed films which clearly indicates that addition of Co to 17 at% leads to strong antiferromagnetic interaction, and above 17 at% ferromagnetic interaction dominates. Moreover, the insertion of Cu-underlayer improves the net magnetization and in-plane magnetic anisotropy of the FePtCo thin films.

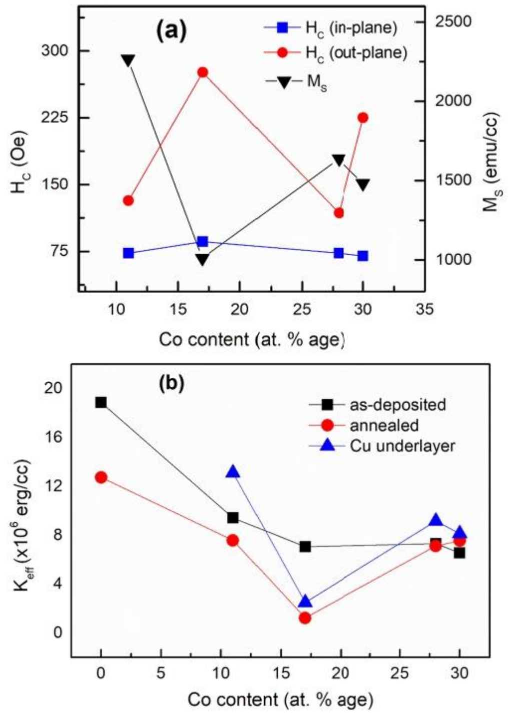

Fig. 12. Plot of variation of (a) H_C and M_S of Cu-under layered films, and (b) K_{eff} of all films deposited under three conditions as a function of Co content of the FePtCo alloy films.

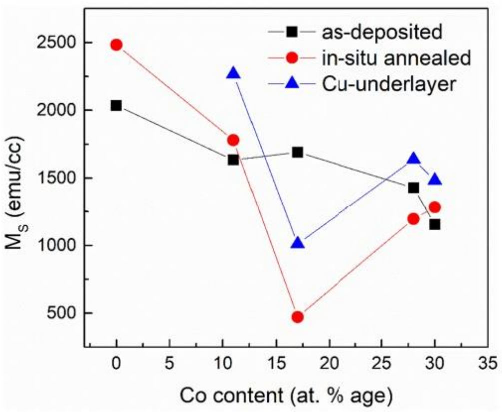

Fig. 13. Plot of saturation magnetization of FePtCo films deposited under three conditions.

5. Conclusion

In conclusion, we have prepared of FePtCo ternary alloy thin films of thickness 100 nm under three deposition conditions as-deposited, in-situ annealed at 673 K, and deposited on 2 nm Cu-underlayer by dc magnetron sputtering. The influence of Co-doping concentration on crystal structure and magnetic properties was studied. Our results showed that all prepared thin films have relatively low surface roughness as measured by 3D optical profilometer and AFM. All films prepared under three deposition conditions crystallized in FCC structure as confirmed by XRD results. The Co addition to FePt leads to reduction in lattice parameters due to smaller atomic radius of Co than Pt. The annealing and insertion of Cu underlayer promotes the crystal growth in (200) and (220) plane. The average crystallite size on the other hand varies with Co content as well as with deposition conditions of the films. All the films prepared under three conditions show soft ferromagnetism and exhibit large in-plane magnetic anisotropy with easy axis parallel to the film plane. The in-plane H_C varies in a smaller range of 46–86 Oe than the out-of-plane H_C (14–931 Oe). The Co addition to FePt leads to an antiferromagnetic coupling between Co and FePt resulting reduction in net magnetization and effective magnetic anisotropy energy constant of as-deposited FePtCo films. On the other hand, an optimum Co addition (17 at%) is observed below which Co addition leads to antiferromagnetic interaction between Co and FePt sublattice for both annealed and Cu under layered films. Above this optimum value, Co addition up to 30 at% leads to ferromagnetic coupling between Co and FePt sublattice, as a result of which saturation magnetization and effective anisotropy constant start increasing. Such interesting magnetic properties of these thin films make them suitable candidate for application in storage devices if properly tuned to achieve perpendicular magnetic anisotropy.

CRediT authorship contribution statement

R. K. Basumatary: Investigation, Methodology, Formal analysis, Writing manuscript; **H. Basumatary:** Investigation, Review & editing; **M. M. Raja**: Investigation, Review & editing; **R. Brahma:** Conceptualization, Methodology, Visualization, Writing – review & editing, Supervision. **S. K. Srivastava:** Conceptualization, Methodology, Visualization, Writing – review & editing, Supervision.

Data availability

Data will be made available on request.

Declaration of Competing Interest

The authors declare that they have no known competing financial interests or personal relationships that could have appeared to influence the work reported in this paper.

Acknowledgements

This present research work is not supported by any kind of research grant. RKB would like to thank DMRL, Hyderabad for helping in characterizing the samples.

References

[1] R.K. Basumatary, B. Aakansha, B. Basumatary, R. Brahma, S. Hussain, R. Ravi, Brahma, S.K. Srivastava, Magnetic property of CoTbNi ternary alloy thin films, J. Supercond. Nov. Magn. 33 (2020) 3165.
[2] R. Hussain, Aakansha, S. Ravi, S.K. Srivastava, Influence of Substrate (Si and Glass), Cu under-Layer, in Situ Annealing of Ta/Cu and Post-Annealing on Magnetic Properties of [Co(0.3 Nm)/Ni(0.6 Nm)]4, 10 Multilayer Thin Films, J. Mater. Sci. Mater. Electron. 31 (2020) 11975.
[3] R. Hussain, Aakansha, B. Brahma, R.K. Basumatary, R. Brahma, S. Ravi, S.K. Srivastava, Sperimagnetism in perpendicularly magnetized Co-Tb alloy-based thin films, J. Supercond. Nov. Magn. 32 (2019) 4027.
[4] R. Hussain, Aakansha, B. Brahma, R. Basumatary, R. Brahma, S. Ravi, S.K. Srivastava, Magnetic property of thin film of Co-Tb alloys deposited on the barrier layer of ordered anodic alumina templates, J. Supercond. Nov. Magn. 33 (2020) 1759.

[5] B. Brahma, R. Hussain, R.K. Basumatary, S. Aakansha, Ravi R. Brahma, S.K. Srivastava, Influence of Cu insertion layer on magnetic properties of Co-Tb/Cu/Co-Tb thin films, J. Supercond. Nov. Magn. 33 (2020) 2891.

[6] S.K. Srivastava, R. Hussain, T. Hauet, L. Piraux, Magnetization reversal and switching field distribution in Co-Tb based bit patterned media, AIP Conf. Proc. 2115 (2019) 1.

[7] B. Brahma, R. Hussain, Aakansha, P. Behera, S. Ravi, R. Brahma, S.K. Srivastava, Tuning the perpendicular magnetic anisotropy of [Co(0.3nm)/Ni(0.6nm)]20 multilayer thin films, Thin Solid Films 728 (2021) 0.

[8] T. Hauet, et al., Reversal mechanism, switching field distribution, and dipolar frustrations in Co/Pt bit pattern media based on auto-assembled anodic alumina hexagonal nanobump arrays, Phys. Rev. B - Condens. Matter Mater. Phys. 89 (2014) 1.

[9] R. Hussain, Aakansha, S. Ravi, S.K. Srivastava, Magnetic properties of ordered array of nanobumps of [Co/Ni]4, 10, 20 multilayers, Solid State Commun. 324 (2021) 114144.

[10] L. Piraux, V.A. Antohe, F. Abreu Araujo, S.K. Srivastava, M. Hehn, D. Lacour, S. Mangin, T. Hauet, Periodic arrays of magnetic nanostructures by depositing Co/Pt multilayers on the barrier layer of ordered anodic alumina templates, Appl. Phys. Lett. 101 (2012).

[11] Y.B. Li, Y.F. Lou, L.R. Zhang, B. Ma, J.M. Bai, F.L. Wei, Effect of magnetic field annealing on microstructure and magnetic properties of FePt films, J. Magn. Magn. Mater. 322 (2010) 3789.

[12] B. Yao, K.R. Coffey, Quantification of L10 phase volume fraction in annealed [Fe/Pt]n multilayer films, J. Appl. Phys. 105 (2009) 0.

[13] J. Park, Y.K. Hong, S.G. Kim, L. Gao, J.U. Thiele, Magnetic properties of Fe-Mn-Pt for heat assisted magnetic recording applications, J. Appl. Phys. 117 (2015) 3.

[14] Y.F. Ding, J.S. Chen, E. Liu, Structural and magnetic properties of FePt films grown on Cr 1-XMox underlayers, Appl. Phys. A Mater. Sci. Process. 81 (2005) 1485.

[15] Y.N. Hsu, S. Jeong, D.E. Laughlin, D.N. Lambeth, Effects of Ag underlayers on the microstructure and magnetic properties of epitaxial FePt thin films, J. Appl. Phys. 89 (2001) 7068.

[16] S.C. Chen, P.C. Kuo, C.Y. Chou, A.C. Sun, Effects of Ag buffer layer on the microstructure and magnetic properties of nanocomposite FePt/Ag multilayer films, J. Appl. Phys. 97 (2005) 10.

[17] J.C.A. Huang, Y.C. Chang, C.C. Yu, Y.D. Yao, Y.M. Hu, C.M. Fu, Mn doping effect on structure and magnetism of epitaxial $(FePt)_{1-x}Mn_x$ films, J. Appl. Phys. 93 (2003) 8173.

[18] Y.K. Takahashi, M. Ohnuma, K. Hono, Ordering process of sputtered FePt films, J. Appl. Phys. 93 (2003) 7580.

[19] M.L. Yan, Y.F. Xu, D.J. Sellmyer, Nanostructure and magnetic properties of highly (001) oriented $L1_0$ *$(Fe_{49}Pt_{51})_{1-x}Cu_x$ Films*, J. Appl. Phys. 99 (2006) 08G903.

[20] M.L. Yan, N. Powers, D.J. Sellmyer, Highly oriented nonepitaxially grown L10 FePt films, J. Appl. Phys. 93 (2003) 8292.

[21] Y.K. Takahashi, M. Ohnuma, K. Hono, Effect of Cu on the structure and magnetic properties of FePt sputtered film, J. Magn. Magn. Mater. 246 (2002) 259.

[22] N.Y. Schmidt, S. Laureti, F. Radu, H. Ryll, C. Luo, F. D'Acapito, S. Tripathi, E. Goering, D. Weller, M. Albrecht, Structural and magnetic properties of FePt-Tb alloy thin films, Phys. Rev. B 100 (2019) 1.

[23] N.Y. Schmidt, R. Mondal, A. Donges, J. Hintermayr, C. Luo, H. Ryll, F. Radu, L. Szunyogh, U. Nowak, M. Albrecht, *$L1_0$ -Ordered $(Fe_{100-x}Cr_x)Pt$ Thin Films: Phase Formation, Morphology, and Spin Structure*, Phys. Rev. B 102 (2020) 1.

[24] G. Meyer, J.U. Thiele, Effective electron-density dependence of the magnetocrystalline anisotropy in highly chemically ordered pseudobinary $(Fe_{1-x}Mn_x)_{50}Pt_{50}$ $L1_0$ alloys, Phys. Rev. B - Condens. Matter Mater. Phys. 73 (2006) 1.

[25] N.Y. Schmidt, S. Abdulazhanov, J. Michalička, J. Hintermayr, O. Man, O. Caha, M. Urbánek, M. Albrecht, Effect of Gd addition on the structural and magnetic properties of L10-FePt alloy thin films, J. Appl. Phys. 132 (2022) 213908.

[26] Y.Z. Zhou, J.S. Chen, G.M. Chow, J.P. Wang, Structure and magnetic properties of in-plane oriented FePt - Ag nanocomposites, J. Appl. Phys. 93 (2003) 7577.

[27] X.H. Xu, H.S. Wu, F. Wang, X.L. Li, Structure and magnetic properties of FePt and FePt/Ag thin films deposited by magnetron sputtering, Thin Solid Films 472 (2005) 222.

[28] D. Weller, G. Parker, O. Mosendz, E. Champion, B. Stipe, X. Wang, T. Klemmer, G. Ju, A. Ajan, *A HAMR Media Technology Roadmap to an Areal Density of 4 Tb/In^2*, IEEE Trans. Magn. 50 (2014).

[29] C. Feng, Q. Zhan, B. Li, J. Teng, M. Li, Y. Jiang, G. Yu, Magnetic properties and microstructure of FePt/Au multilayers with high perpendicular magnetocrystalline anisotropy, Appl. Phys. Lett. 93 (2008) 10.

[30] M. Maret, C. Brombacher, P. Matthes, D. Makarov, N. Boudet, M. Albrecht, *Anomalous X-Ray Diffr. Meas. Long. -Range Order (001)-Texture L1 0 FePtCu Thin Films*, Phys. Rev. B - Condens. Matter Mater. Phys. 86 (2012) 1.

[31] R. Cuadrado, T.J. Klemmer, R.W. Chantrell, *Magnetic Anisotropy of $Fe_{1-y}X_yPt$-$L1_0$ [X = Cr, Mn, Co, Ni, Cu] Bulk Alloys*, Appl. Phys. Lett. 105 (2014) 0.

[32] T. Ono, H. Nakata, T. Moriya, N. Kikuchi, S. Okamoto, O. Kitakami, T. Shimatsu, Experimental Investigation of Off-Stoichiometry and 3d Transition Metal (Mn, Ni, Cu)-Substitution in Single-Crystalline FePt Thin Films, AIP Adv. 6 (2016) 6.

[33] C. Brombacher, H. Schletter, M. Daniel, P. Matthes, N. Jöhrmann, M. Maret, D. Makarov, M. Hietschold, M. Albrecht, *FePtCu Alloy Thin Films: Morphology, $L1_0$ Chemical Ordering, and Perpendicular Magnetic Anisotropy*, J. Appl. Phys. 112 (2012).

[34] A. Asthana, Y.K. Takahashi, Y. Matsui, K. Hono, Effect of base pressure on the structure and magnetic properties of FePt thin films, J. Magn. Magn. Mater. 320 (2008) 250.

[35] M.E. Gruner, P. Entel, Structural and magnetic properties of ternary Fe1-XMnxPt nanoalloys from first principles, Beilstein J. Nanotechnol. 2 (2011) 162.

[36] T. Burkert, O. Eriksson, S.I. Simak, A.V. Ruban, B. Sanyal, L. Nordström, J.M. Wills, *Magnetic Anisotropy of $L1_0$ FePt and $Fe_{1-x}Mn_xPt$*, Phys. Rev. B - Condens. Matter Mater. Phys. 71 (2005) 1.

[37] D.B. Xu, C.J. Sun, J.S. Chen, S.M. Heald, B. Sanyal, R.A. Rosenberg, T.J. Zhou, G.M. Chow, Large Enhancement of Magnetic Moment in L10 Ordered FePt Thin Films by Nd Substitutional Doping, J. Phys. D. Appl. Phys. 48 (2015).

[38] F. Rafieian, M. Mousavi, A. Dufresne, Q. Yu, Polyethersulfone Membrane Embedded with Amine Functionalized Microcrystalline Cellulose, Int. J. Biol. Macromol. 164 (2020) 4444.

[39] K. Sin, J.M. Sivertsen, J.H. Judy, Surface roughness and magnetic properties of in situ heated and postannealed thin films of perpendicular barium ferrite, J. Appl. Phys. 75 (1994) 5972.

[40] R. Dinnebier, *Rietveld Refinement Powder Diffr. Data*, Vol. Dec. 2 (2001).

[41] B. Samantaray, S. Ravi, et al., Magnetic structure and magnetic properties of $Nd_{1-x}Na_xMnO_3$ compounds, J. Appl. Phys. 110 (2011) 093906.

[42] S.K. Srivastava, M. Kar, S. Ravi, Effect of Co doping on the magnetic properties of La0.85Ag0.15(Mn1-yCoy)O3, J. Magn. Magn. Mater. 32 (2008) 107.

[43] E. Clementi, D.L. Raimondi, W.P. Reinhardt, Atomic screening constants from SCF functions. II. Atoms with 37 to 86 electrons, J. Chem. Phys. 47 (1967) 1300.

[44] R. Yogamalar, R. Srinivasan, A. Vinu, K. Ariga, A.C. Bose, X-ray peak broadening analysis in ZnO nanoparticles, Solid State Commun. 149 (2009) 1919.

[45] S. Mustapha, M.M. Ndamitso, A.S. Abdulkareem, J.O. Tijani, D.T. Shuaib, A. K. Mohammed, and A. Sumaila, *Comparative Study of Crystallite Size Using Williamson-Hall and Debye-Scherrer Plots for ZnO Nanoparticles*, Adv. Nat. Sci. Nanosci. Nanotechnol. 10 (2019).

[46] U. Holzwarth, N. Gibson, The scherrer equation versus the "debye-scherrer equation, Nat. Nanotechnol. 6 (2011) 534.

[47] H. Gao, T. Harumoto, W. Luo, R. Lan, H. Feng, Y. Du, Y. Nakamura, J. Shi, Room temperature perpendicular exchange bias in CoNi/(Co,Ni)O multilayers with perpendicular magnetic anisotropy directly induced by FM/AFM interface, J. Magn. Magn. Mater. 473 (2019) 490.

Journal of Superconductivity and Novel Magnetism (2020) 33:3165–3170
https://doi.org/10.1007/s10948-020-05574-3

ORIGINAL PAPER

Magnetic Property of CoTbNi Ternary Alloy Thin Films

R. K. Basumatary [1] · Aakansha [2] · B. Basumatary [3] · B. Brahma [1,4] · R. Hussain [4] · S. Ravi [2] · R. Brahma [1] · S. K. Srivastava [4]

Received: 4 April 2020 / Accepted: 10 June 2020 / Published online: 18 June 2020

Abstract

The structure and magnetic property of as prepared and post-annealed thin films of CoTbNi ternary alloy have been investigated. $(Co_{0.85}Tb_{0.15})_{1-x}Ni_x$ alloy thin films with $x = (0.54, 0.63, 0.72, 0.81)$ were grown on Si-substrate by co-sputtering of Ni element and $Co_{0.85}Tb_{0.15}$ alloy using dc magnetron sputtering. These films have been crystallized in amorphous form, as confirmed by X-ray diffraction (XRD) measurement. The magnetization versus field measurements shows that these films exhibit room temperature ferromagnetism. The magnetic properties of these alloy films have a strong dependency on the Ni concentrations. It is observed that the saturation magnetization and coercivity of these alloy thin films decreases with increase of Ni content of the films. One of the striking features was the observation of perpendicular magnetic anisotropy (PMA) for $x = 0.63$ and 0.72 thin films. However, the observed PMA disappears upon post-annealing of the films. The M-T measurement shows that the ferromagnetic transition temperatures of these materials are much higher than the room temperature.

Keywords Thin film · Ternary CoTbNi alloy · Co-Tb alloy · Perpendicular magnetic anisotropy

1 Introduction

Since last couple of decades, there have been intense investigations on the magnetic properties of amorphous rare-earth-transition metal (RE-TM) thin films due to their potential applications in various practical devices such as spintronic and perpendicular magnetic recording devices. The RE-TM alloys are usually ferrimagnetic with the moments of RE (Gd, Tb, Ho, etc.) and TM (Fe, Co, Ni, etc.) aligned antiparallel due to the exchange interaction between *f* and *d* electrons [1, 2]. The magnetic properties of these alloy films can be tuned by the addition of under- and/or over-layers, such as Cu, Al, Ag, TiN, Ta, etc. which also can serve as protective layer for oxidation and coercivity enhancement [3–7]. The other way to modify the magnetic properties of RE-TM alloy films is by varying film composition, film thickness, sputtering conditions, and microstructure [8–10].

Recently, the discovery of perpendicular magnetic anisotropy (PMA) in amorphous Co-Tb-based alloys have been revisited by the investigators due to their wide variety of collinear magnetic ordering such as ferrimagnetism as well as non-collinear magnetic ordering such as speromagnetism, asperomagnetism, and sperimagnetism, which occur due to competition between random local anisotropy and exchange interaction [11–16]. Co-Tb-based alloys have high perpendicular magnetic anisotropy and low magnetization which make these alloys a potential candidate for data storage application. One advantage of using such low magnetization materials for data storage is its weak coupling to any external magnetic field that could otherwise erase the stored information. Magnetic anisotropy is also the origin of long-range magnetic order in low dimensional magnetic systems [17] that play a vital role in determining the magnetically hard and soft properties of a material [18]. In our previous report, PMA along with biaxial anisotropy was observed in $Co_{0.85}Tb_{0.15}$ film with coercive field of 600 Oe [13]. Moreover, it was reported by Tang et al. that PMA strength decreases in both Co-rich and Tb-rich CoTb alloy films [19]. In the present work, we have taken

✉ S. K. Srivastava
sk.srivastava@cit.ac.in

1 Department of Physics, Bodoland University, Kokrajhar 783370, India

2 Department of Physics, Indian Institute of Technology Guwahati, Guwahati 781039, India

3 Physical Science Division, Institute of Advanced Study in Science and Technology, Guwahati 781035, India

4 Department of Physics, Central Institute of Technology Kokrajhar, Kokrajhar 783370, India

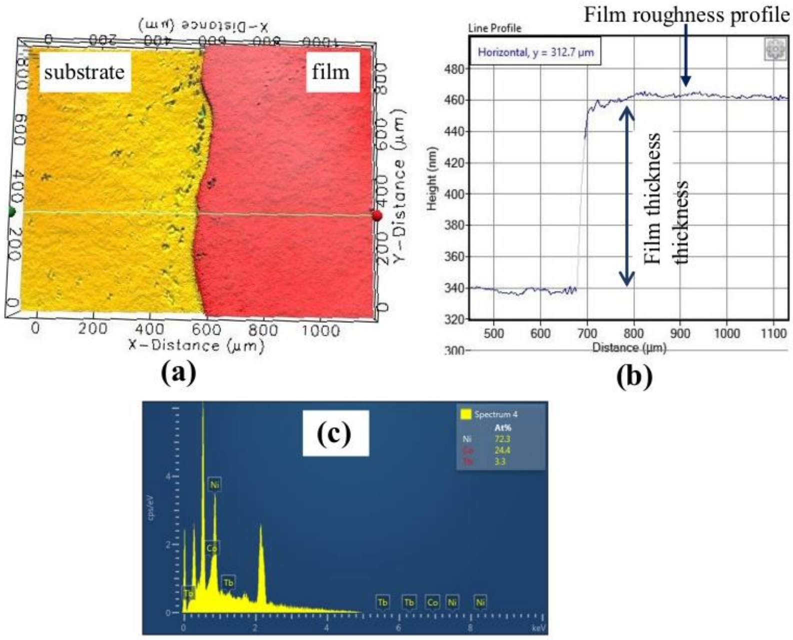

Fig. 1 **a** Top view of the step height and surface roughness of $(Co_{0.85}Tb_{0.15})_{0.46}Ni_{0.54}$ film captured by profilm 3D filmetrics optical profilometer. The left portion (yellow) of **a** is the substrate while the right portion (red) is film. **b** Film thickness and surface roughness profile of deposited film. **c** EDX spectrum for $x = 0.72$ sample

up to study the Ni-rich CoTbNi alloy thin films and to see its influence on the crystal structure and magnetic property. We also study the effect of post annealing on magnetic properties of these alloy films.

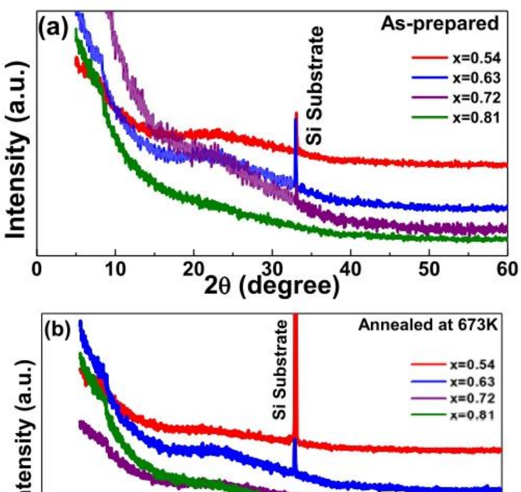

Fig. 2 XRD pattern of **a** as-prepared and **b** post-annealed thin films of $(Co_{0.85}Tb_{0.15})_{1-x}Ni_x$ ($x = 0$, 0.54, 0.63, 0.72, 0.81) alloy

2 Experimental Details

Four samples of $(Co_{0.85}Tb_{0.15})_{1-x}Ni_x$ alloy thin films with $x = (0.54, 0.63, 0.72, 0.81)$ have been prepared by co-sputtering of $Co_{0.85}Tb_{0.15}$ and pure Ni targets on Si substrate under high vacuum (base pressure ~4×10^{-5} mbar) using DC magnetron sputtering system. During co-sputtering, the $Co_{0.85}Tb_{0.15}$ target was deposited at constant power in all the samples and the pure Ni target was deposited at four different power to vary the Ni content in all the samples. The total thickness of all CoTbNi ternary alloy films were kept constant (120 nm). A non-magnetic layer of Ta (2 nm thick) has also been deposited as a cap layer to protect the film from oxidation and scratches. A set of four samples with same compositions were deposited and annealed at 400 °C for 1 h to study the effect of post-annealing on the magnetic properties of these samples. The film thickness and film roughness of all prepared films were measured by 3D optical profilometer (3D profilm, Filmetrics). The structural analyses were carried out by X-ray diffraction measurement. The film compositions were determined by energy-dispersive X-ray spectroscopy, and the magnetic properties were measured by vibrating sample magnetometer (VSM).

3 Results and Discussion

The film thickness and surface roughness of the deposited $(Co_{0.85}Tb_{0.15})_{1-x}Ni_x$ alloy films were measured by 3D optical

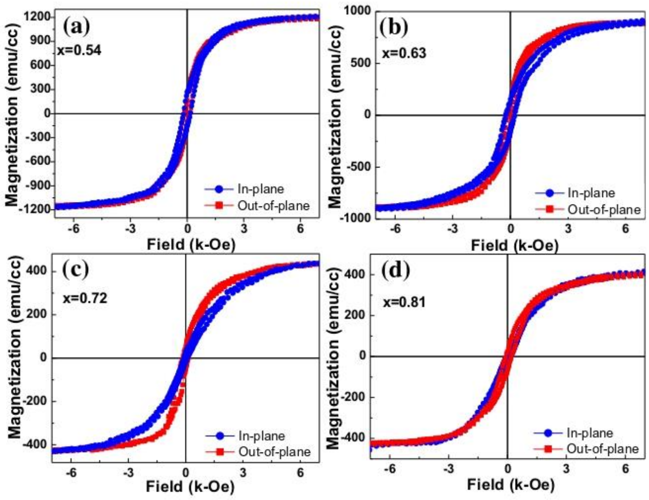

Fig. 3 **a–d** Out-of-plane (solid squire) and in-plane (solid circle) M-H curves for as-prepared $(Co_{0.85}Tb_{0.15})_{1-x}Ni_x$ alloy films measured at room temperature

profilometer. To measure the film thickness and to study the surface profile of prepared films, a step height was created by depositing the thin films on a partially masked substrate. After deposition, the mask was removed and step height was measured. The top view of a typical step height has been presented in Fig. 1a. The average roughness of the film is recorded to be ~ 4 nm, which indicates that the films are relatively smooth (see Fig. 1b). The compositions of all prepared $(Co_{0.85}Tb_{0.15})_{1-x}Ni_x$ alloy films were estimated by energy-dispersive X-ray spectroscopy (EDS). The composition of the samples is found to be $x = 0.54$, 0.63, 0.72, 0.81. Typical EDS spectrum of $x = 0.72$ sample is presented in Fig. 1c. The structural analyses of the as-prepared and post-annealed films of these alloys were carried out by XRD measurement and presented in Fig. 2. The annealing of samples was carried out at 400 °C, the temperature at which formation of crystalline phase starts for CoTb alloy film [20]. The X-ray patterns for both as-prepared and annealed samples show a broad maximum, typically observed for amorphous alloys, as described in other work [13]. Additionally, a crystalline peak has been observed at $2\theta \sim 33°$ for both as-prepared sample and post-annealed films. This narrow reflection is likely due to Si (100) substrates, which is usually observed in XRD measurements of different materials deposited on Si (100) substrates. No evolution of other peaks is observed with increasing Ni content in as-prepared as well as in annealed samples. It indicates that crystalline temperature for these alloys is above the 400 °C.

The measurement of in-plane and out-of-plane magnetization (M) as a function of magnetic field (H) for all the prepared $(Co_{0.85}Tb_{0.15})_{1-x}Ni_x$ alloy films have been carried out using VSM at room temperature. The in-plane M-H curves were measured with application of field parallel to the film plane and out-of-plane M-H curves were measured with field perpendicular to the film plane. The well-defined in-plane and out-plane M-H hysteresis loop of as-prepared samples as shown in Fig. 3a–d indicate that all the samples exhibit room temperature ferromagnetism. It is observed that saturation magnetization (M_s) and squareness [M_R/M_S] were found to

Table 1 Variation of magnetic properties parameters of $(Co_{0.85}Tb_{0.15})_{1-x}Ni_x$ alloy films with $x = (0.54, 0.63, 0.72, 0.81)$. H_C is perpendicular coercivity. M_R and M_S are the remanent and saturation magnetization, respectively. [M_R/M_S] indicates squareness of the hysteresis curves. K_{eff} is the effective anisotropy constant

Parameters	Samples							
	$x = 0.54$		$x = 0.63$		$x = 0.72$		$x = 0.81$	
	As-pre.	Post-ann.	As-pre.	Post-ann.	As-pre.	Post-ann.	As-pre.	Post-ann.
H_C (Oe)	140	149	141	145	145	148	150	150
M_R (emu/cc)	134	42	95	82	44	72	23	56
M_S (emu/cc)	1170	764	890	805	431	351	399	368
[M_R/M_S]	0.11	0.05	0.11	0.10	0.10	0.20	0.06	0.15
K_{eff} (erg/cm^3)	–		2.42×10^6		1.57×10^6		–	

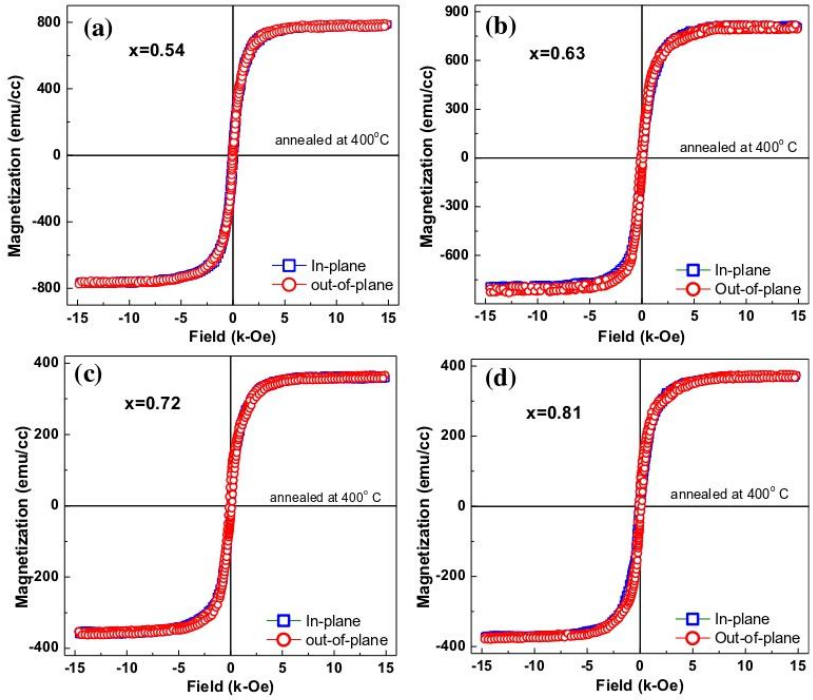

Fig. 4 **a**–**d** Out-of-plane (red) and in-plane M-H curves for annealed $(Co_{0.85}Tb_{0.15})_{1-x}Ni_x$ alloy films measured at room temperature. Annealing of thin film was carried out at 400 °C

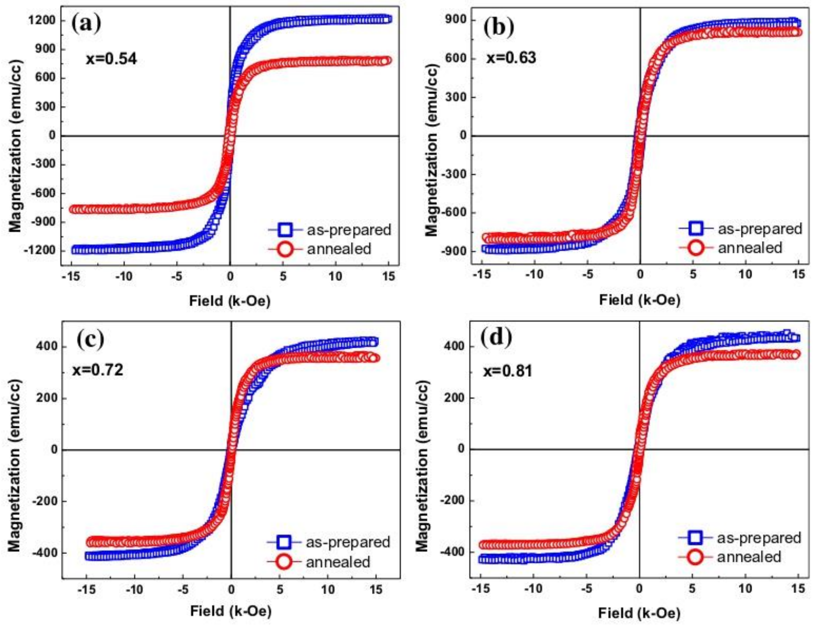

Fig. 5 Comparative plot of out-plane M-H curves for as-prepared (blue) and post-annealed samples (red) measured at room temperature with field applied in direction of plane of the film

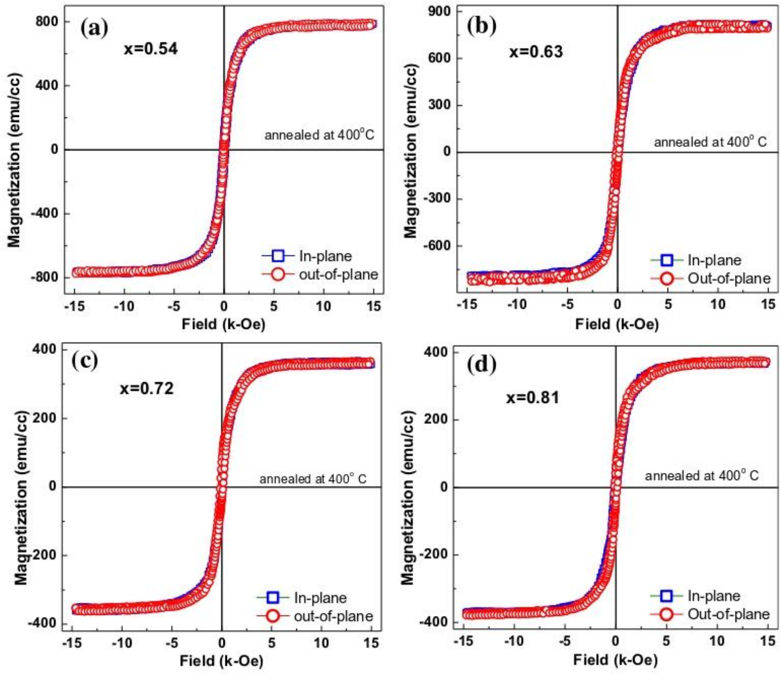

Fig. 4 **a–d** Out-of-plane (red) and in-plane M-H curves for annealed $(Co_{0.85}Tb_{0.15})_{1-x}Ni_x$ alloy films measured at room temperature. Annealing of thin film was carried out at 400 °C

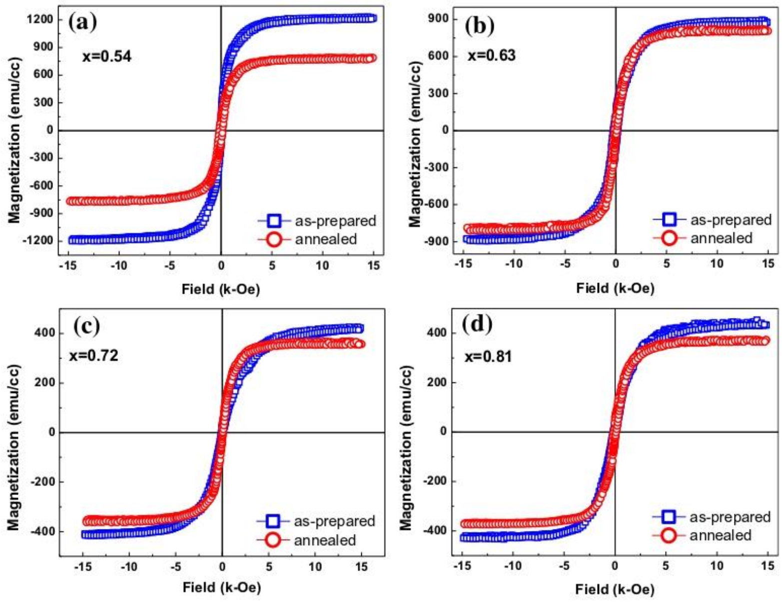

Fig. 5 Comparative plot of out-plane M-H curves for as-prepared (blue) and post-annealed samples (red) measured at room temperature with field applied in direction of plane of the film

Acknowledgments SKS acknowledges the financial support for a project through "Early Career Research Award" from DST-SERB India, with sanction order number (ECR/2016/000713).

References

1. Campbell, A.: J. Phys. **F2**, L47–L50 (1972)
2. Becker, J., Tsukamoto, A., Kirilyuk, A., Maan, J.C., Rasing, T., Christianen, P.C.M., Kimel, A.V.: Phys. Rev. Lett. **118**, 117203 (2017)
3. Miyanishi, S., Kojima, K., Sato, J., Takayama, K., Fuji, H., Takahashi, A., Ohta, K.: J. Appl. Phys. **93**, 7801–7803 (2003)
4. Ito, H., Song, K., Naoe, M.: J. Appl. Phys. **79**, 6273–6275 (1996)
5. Sato, J., Murakami, Y., Fuji, H., Kojima, K., Takahashi, A., Nakatani, R., Yamamoto, M.: Jpn. J. Appl. Phys. **47**, 150–153 (2008)
6. Fang, Y.H., Kuo, P.C., Chou, C.Y., Chen, S.C., Cheng, N.W., Lin, P.L.: J. Magn. Magn. Mater. **310**, e930–e932 (2007)
7. Rahman, M.T., Liu, X., Morisako, A.: J. Magn. Magn. Mater. **303**, e133–e136 (2006)
8. Takagi, H., Tsunashima, S., Uchiyama, S.: J. Appl. Phys. **50**, 1642–1644 (2008)
9. Nihara, T., Takayama, S., Sugita, Y.: IEEE Trans. Magn. **MAG-21**, 1638–1640 (1985)
10. Umadevi, K., Bysakh, S., Chelvane, J.A., Kamat, S.V., Jayalakshmi, V.: J. Alloys Compd. **663**, 430–435 (2016)
11. Moorjani, K., Coey, J.M.D.: Magnetic Glasses, pp. 210–218. Elsevier, Amsterdam (1984)
12. Hansen, P.: In: Buschow, K.H.J. (ed.) Handbook of Magnetic Materials, vol. 6, pp. 315–319. North-Holland, Amsterdam (1991)
13. Hussain, R., Aakansha, B., Brahma, R., Basumatary, K., Brahma, R., Ravi, S., Srivastava, S.K.: J. Supercond. Nov. Magn. **32**, 4027–4031 (2019)
14. Hussain, R., Aakansha, B., Brahma, R., Basumatary, R., Brahma, S., Ravi, S.K.: Srivastava. J. Supercond. Nov. Magn. **33**, 1759–1763 (2020)
15. Srivastava, S.K., Hussain, R., Hauet, T., Piraux, L.: AIP Conf. Proc. **2115**, 030482 (2019)
16. Brahma, B., Hussain, R., Basumatary, R.K., Aakansha, Ravi, S., Brahma, R., Srivastava, S.K.: J. Superconduct. Novel Magn. (2020). https://doi.org/10.1007/s10948-020-05556-5
17. Bander, M., Mills, D.L.: Phys. Rev. B. **38**, 12015–12018 (1988)
18. Wang, S.X., Sun, N.X., Yamaguchi, M., Yabukami, S.: Nature. **407**, 150–151 (2000)
19. Tang, M., Chen, S., Zhang, X., Zhang, Z., Jin, Q.Y.: SPIN. **6**, 1650009 (2016)
20. Soltani, M.L.: J. Non Cryst. Solids. **353**, 2074–2078 (2007)
21. Yan, X., Hirscher, M., Egami, T.: Phys. Rev. B. **43**, 9300–9303 (1991)
22. Hindmarch, A.T., Rushforth, A.W., Campion, R.P., Marrows, C.H., Gallagher, B.L.: Phys. Rev. B. **83**, 212404 (2011)

174 (2023) 207491

Contents lists available at ScienceDirect

Micro and Nanostructures

journal homepage: www.journals.elsevier.com/micro-and-nanostructures

Influence of surface roughness on magnetic properties of CoTbNi ternary alloy films

R.K. Basumatary [a,b], P. Behera [c], B. Basumatary [d], B. Brahma [e], S. Ravi [c], R. Brahma [a,*], S.K. Srivastava [e,**]

[a] Department of Physics, Bodoland University, Kokrajhar, 783370, India
[b] Department of Physics, Darrang College, Tezpur, 784001, India
[c] Department of Physics, Indian Institute of Technology Guwahati, Guwahati, 781039, India
[d] Physical Science Division, Institute of Advanced Study in Science and Technology, Guwahati, 781035, India
[e] Department of Physics, Central Institute of Technology Kokrajhar, Kokrajhar, 783370, India

ARTICLE INFO

Keywords:
Ternary alloy
Thin films
Ferromagnetism
Surface roughness
Rare earth transition metal

ABSTRACT

Rare earth-transition metal (RE-TM) amorphous alloys films with promising tunable perpendicular magnetic anisotropy are projected to be exploited for magnetic recording media and spintronic applications. Here variation of magnetic property of thin films of $Co_{0.63}Tb_{0.11}Ni_{0.26}$, $Co_{0.41}Tb_{0.14}Ni_{0.45}$ and $Co_{0.32}Tb_{0.08}Ni_{0.60}$ ternary alloy fabricated on Si-substrate using dc magnetron sputtering at room temperature were studied. The x-ray diffraction pattern data confirms the amorphous nature of these alloy films. The average surface roughness (S_a and R_a) of the films is found to vary significantly with Ni content of the films. The room temperature field dependent magnetization measurement shows the room temperature ferromagnetism. The saturation magnetization and coercivity of the *M*-H curves are found to vary with Ni content as well as surface roughness of the films. However, the nature of variation of saturation magnetization and coercive field is in accordance with variation of surface roughness, indicating that film surface roughness play a vital role in tuning the magnetic properties of these thin films. Such tunable magnetic properties of these amorphous films make them good candidate for magnetic storage media applications.

1. Introduction

Since the last decades, intense research has been carried out on magnetic materials for various practical applications like magnetic memories, spintronics, GMR spin-valve system for read/write head, micro-actuator, etc. Permalloys have been known to be the best iron group thin films for application in magnetic recording systems and microelectromechanical systems with high saturation field and low coercivity [1–5]. Various CoFe and CoNi-based ternary alloy films like TbCoFe [6], CoFeCu [2], CoFeNi [7,8], CoFeP [9], CoFeSnP [9] and multilayers such as Co/Pt, Co/Ni, Co-Tb [10–18], etc. Have been intensely investigated. For such applications, soft magnetic materials with high saturation field and low coercivity are desired to beat the dramatic increase of the areal density of recording media and for better performance. Recently amorphous rare-earth transition-metal (RE-TM) alloys have attracted the attention of researchers

* Corresponding author.
** Corresponding author.
E-mail addresses: rajibhcu@gmail.com (R. Brahma), sk.srivastava@cit.ac.in (S.K. Srivastava).

https://doi.org/10.1016/j.micrna.2022.207491
Received 13 June 2022; Received in revised form 17 December 2022; Accepted 19 December 2022
Available online 20 December 2022

due to their various interesting properties. These amorphous RE-TM alloy films exhibit ferrimagnetism with moments of RE-sublattice and TM-sublattice antiparallel alignment due to exchange interaction between *5f*-electrons of RE and *3d*-electrons of TM [19,20]. The magnetic property of these alloy films is sensitive to various parameters like film thickness, film composition, sputtering conditions as well as microstructure [21,22]. Interestingly magnetic properties of these alloy films can also be manipulated by inserting non-magnetic layers such as Cu, Al, Ag, Ta, etc. As under-layer and/or over-layer [23–27]. Recently, perpendicular magnetic

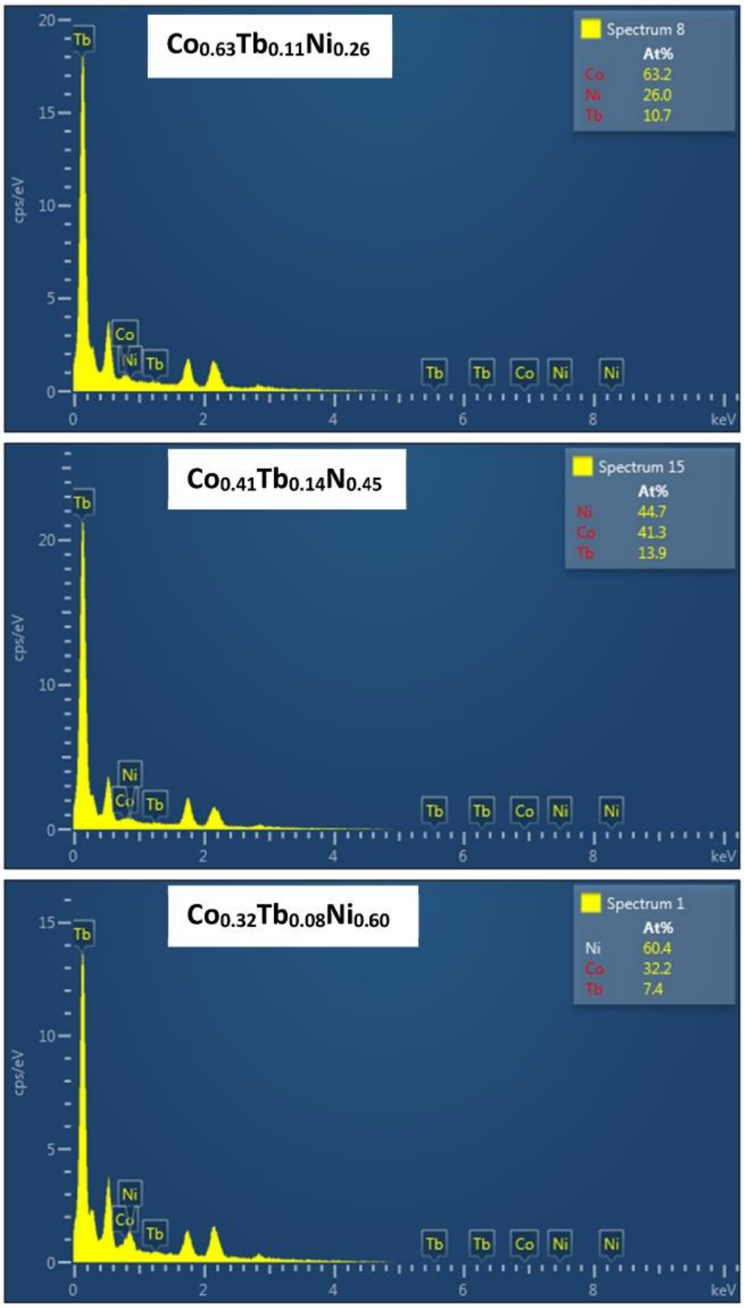

Fig. 1. Energy dispersive spectra of $Co_{1-x-y}Tb_xNi_y$ ternary alloy thin films measured by SEM-EDS.

anisotropy (PMA) has been discovered in amorphous Tb–Co based RE-TM alloy films occurring as a result of competition between exchange interaction and random local anisotropy [28–31]. Biaxial PMA has also been reported in amorphous $Co_{0.85}Tb_{0.15}$ film with the coercive field of 600 Oe [30]. The strength of PMA of CoTb alloy films decreases with the thickness of under-layers [32]. Additionally, the magnetic properties; such as the coercivity, saturation magnetization and remanent magnetization of various ternary alloy and binary alloy films as well as bi-layer films are reported to be strongly influenced by film surface roughness [33–48]. Cao et al. reported the influence of film thickness and surface roughness of magnetron sputtered FeNiCr films [34]. They found that the in-plane coercivity of FeNiCr films increases in a similar manner as the film surface roughness increases [34]. Swerts et al. studied the interplay between surface roughness and magnetic properties of Ag/Fe bilayer films of varying thickness and showed that the coercivity increases with an increase in film surface roughness [35]. They also showed that the film surface characteristics also influence the

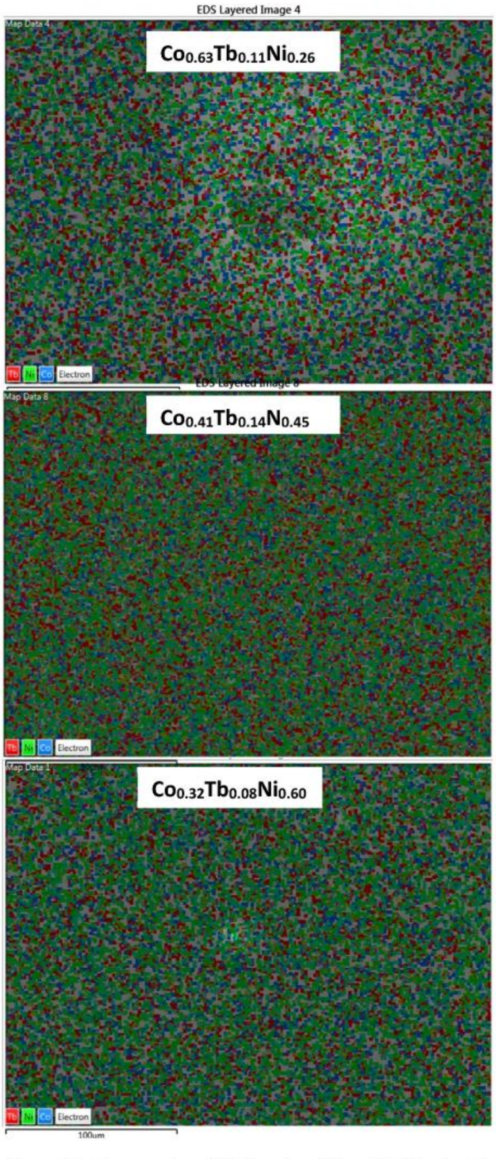

Fig. 2. Elemental colour mapping of EDS spectra of $Co_{1-x-y}Tb_xNi_y$ alloy thin films.

magnetization reversal process. One of the key factors from which coercive force arises in RE-TM amorphous films is the interaction between domain wall and features in the film such as impurities, density fluctuation, surface roughness, etc. On the scale of wall width which act as pinning centers [35,36,38]. Swerts et al. were able to produce artificially modulated magnetic domain configurations by varying the film surface roughness [39]. Also by changing the film thickness they were able to trap the domain wall. Vilain et al. also showed that the remanent magnetization of NiCo films varies nearly parabolic with increase in surface roughness [40]. The roughness of underlayer is also reported to influence the coercivity of RE-TM alloy films such as GdFeCo and TbFeCo by introducing more pinning sites that impede the domain wall movements [41,42]. Katayama et al. studied the effect of Al-underlayer of laser-assisted TbFeCo magnetic recording media and found that the coercivity of non-underlayered films remains the same but it increases for Al-under-layered films which are closely related to the interface roughness of the underlayer [43]. They also observed that the magnetization reversal process of Al underlayered films shifts from wall motion mode to a rotational mode. Such magnetization reversal shifting process is closely attributed to the pinning of domain wall motion due to underlayer surface roughness. The change in magnetic anisotropy of under layered TbFeCo films has also been observed due to the interface roughness [44,45] due to the fact that a flatter interface is usually found to deteriorate the PMA of a thin magnetic layer [42,46]. Similar results were also observed by Tang et al. in under layered TbCo films where perpendicular coercivity increased with surface roughness [47]. Recently, the correlation of film surface roughness to the coercivity of amorphous GdFe films has been reported by Talapatra et al. [48] and Basumatary et al. [38]. Though several researchers have reported the influence of film surface roughness on magnetic properties, these studies were done on films of varying compositions and thicknesses. As a result, the actual dependency of the magnetic property on surface roughness by keeping other parameters of film (thickness, composition) the same were not taken into consideration. In the present work, we attempt to investigate the influence of surface roughness on the magnetic properties of RE-TM CoTbNi ternary alloy thin films by depositing films of same thickness. Our study demonstrates the influence of film surface roughness on saturation magnetization and coercivity of CoTbNi ternary alloy films of same thickness.

2. Experimental details

Ternary alloy thin films of CoTbNi have been prepared using co-sputtering of $Co_{85}Tb_{15}$ and pure Ni target using a dc magnetron sputtering system (Make: Mansha Vacuum Private Limited Bangalore, India). The $Co_{85}Tb_{15}$ target was sputtered at constant power (261 W) for all samples and the Ni target was sputtered at three different power (293, 315, 338 W) to vary the Ni content of the thin film. The deposition was carried out at room temperature at a base pressure of 6.5×10^{-3} Pa and the working pressure of 3 Pa using a DC magnetron sputtering under Ar gas (flow = 5 sccm) environment. A nonmagnetic Ta overlayer of thickness 2 nm was also deposited as a protective layer to prevent the film from oxidation and scratches. The deposition rate (thickness/minute) of each target at each sputtering power was determined before depositing the films of the ternary alloys. The thickness of the films was measured by creating step height by depositing films on partially masked substrates using 3D optical profilometer (Make: Filmetrics USA, Model: profilm). The total thickness of all the thin films was maintained the same by varying the deposition time. Moreover, the film roughness and surface topography were also investigated by 3D optical profilometer. The composition of the films in relative atomic percentage was estimated by energy dispersive x-ray spectroscopy (Make: Zeiss, Model Sigma). The structural analyses of all films were carried out using X-ray diffractometer (Make: RIGAKU, Model: TTRX III) employing CuKα radiation beam using in θ–2θ Bragg-Brentano goniometer geometry and with a step of 0.02°. Room temperature magnetization (M) versus Field (H) measurements were done at room temperature using a vibrating sample magnetometer (Make: Lakeshore, USA).

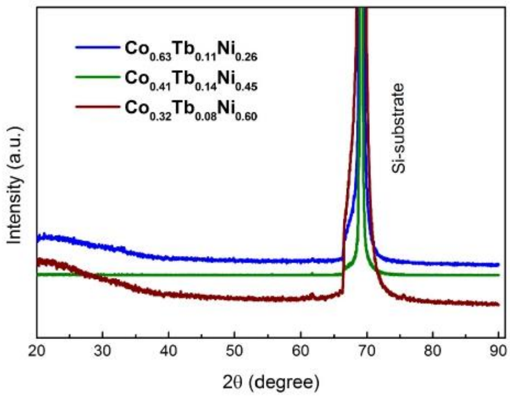

Fig. 3. Room temperature X-ray diffraction pattern of $Co_{1-x-y}Tb_xNi_y$ ternary alloy thin films deposited on Si substrate.

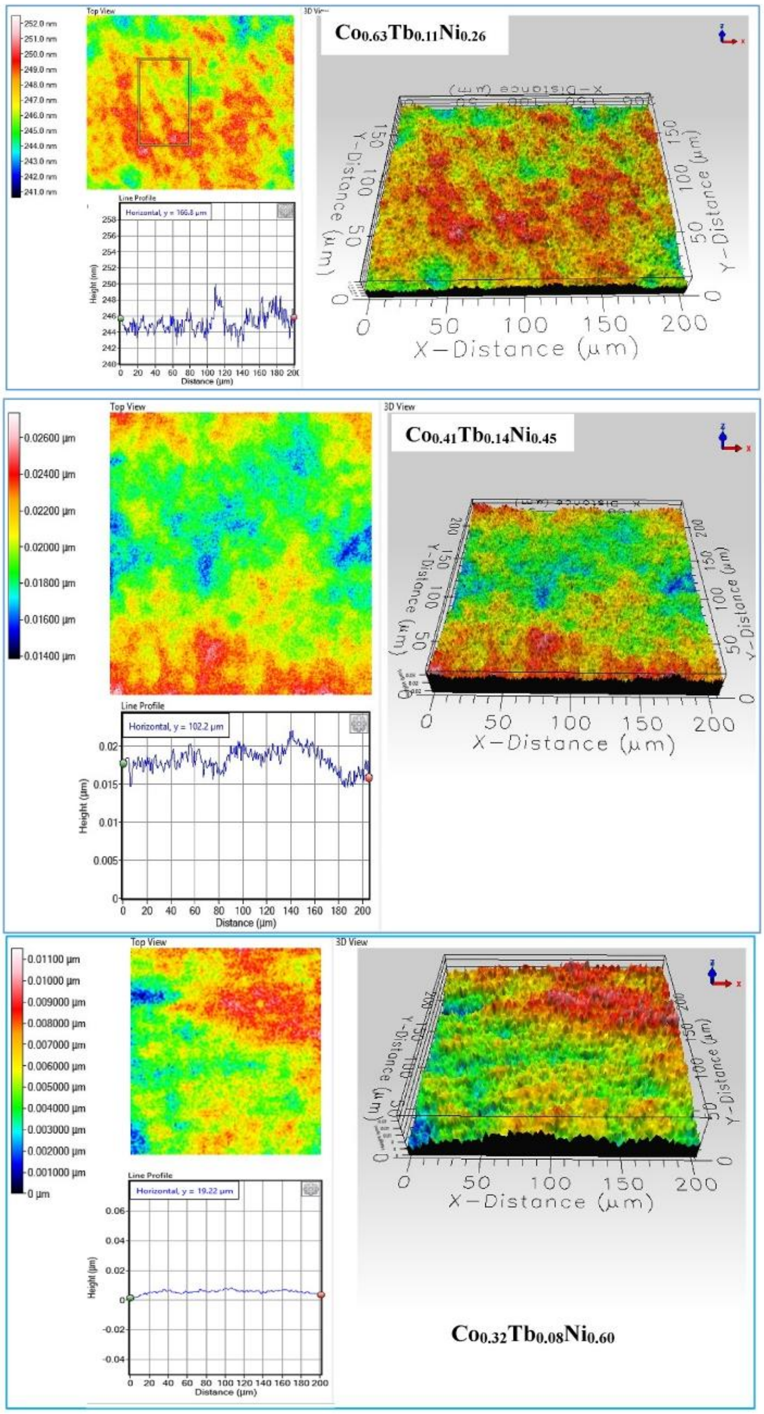

(caption on next page)

Fig. 4. 3D image of Surface topography with colour contrast z-scale and line profile of $Co_{1-x-y}Tb_xNi_y$ alloy films.

3. Results and discussion

The composition of the prepared $Co_{1-x-y}Tb_xNi_y$ films was estimated using EDS. The EDS spectra for all prepared films with the relative atomic percentages of elements present have been presented in Fig. 1. The composition of the films was found to be $Co_{0.63}Tb_{0.11}Ni_{0.26}$, $Co_{0.41}Tb_{0.14}Ni_{0.45}$ and $Co_{0.32}Tb_{0.08}Ni_{0.60}$. The Ni content of the films increases with an increase in Ni target sputtering power as expected. Moreover, to ensure that the deposition has taken place uniformly, we have carried out the elemental colour mapping of the films using EDS. Fig. 2 indicates the elemental colour mapping of the EDS spectrum of the prepared thin films. The films are found to be uniform and homogeneous as evidenced by the elemental colour mapping by EDS spectra.

The structural analyses of all films were carried out by room temperature XRD measurement using Cu-$K\alpha$ radiation. The obtained XRD profile of the films is illustrated in Fig. 3. The intense peak at $2\theta = 69.23^\circ$ is a reflection of Si (400) substrate which is confirmed by comparing it to JCPDS card no. 27–1402. No evolution of other XRD peaks with an increase in the Ni-content of the films is observed. The broad maxima observed below $2\theta = 40^\circ$ is the signature of amorphous materials as described in Refs. [14,30,39,49]. This observation confirms the amorphous nature of the deposited films. The film thickness and surface roughness were estimated by 3D optical profilometer filmetrics. In order to measure the film thickness, each film was deposited on a partially masked substrate for 30 min. After deposition, the masks were removed and the step heights were measured and the deposition rate per minute in terms of thickness per minute was determined. The actual thin films were then deposited to maintain the overall thickness ~ 120 nm. The 3D surface topography was measured using profilm 3D (filmetrics) optical profilometer. The surface roughness parameters S_a and R_a were estimated using ISO 25178 Height and ISO 4287 Amplitude standards respectively using profilm 3D integrated software. S_a is the average absolute distances of the surface points from the mean plane [50]. On the other hand, R_a is the average deviation of the roughness profile within the scanned length of the sample [51]. The digital equation by which S_a [50] and R_a [51] are calculated are

$$S_a = \frac{1}{MN}\sum_{j=1}^{N}\sum_{i=1}^{M}\left|Z\left(x_i, y_j\right)\right|$$

$$R_a = \frac{1}{l}\int_0^l Z(x)dx$$

Where M and N are the number columns and rows on the surface and l is the sampling length of the sample. The 3D images of surface topography with colour contrast z-scale and line profile of all prepared alloy thin films are presented in Fig. 4. The obtained film thickness and the average surface roughness S_a are illustrated in Table 1. The S_a of the films is found to first increase from 1.083 nm for 26% Ni-doped film to 1.632 nm for 45% Ni-doped and then decreases to 1.376 nm for 60% Ni-doped thin film. The value of R_a slightly varies from point to point of the sample within the scan area. So for the best results, the R_a is estimated at the center of the sample within the scan area. The value of R_a also varies with composition of the films in similar pattern as S_a. The value of R_a also first increases from 0.463 nm for 26% Ni-doped film to 0.735 nm for 45% Ni-doped film and then decreases to 0.487 nm for 60% Ni-doped thin films (Fig. 7 (a) and (b)).

The measurement of magnetization as a function of magnetic was carried out at room-temperature using VSM and presented in Fig. 6. The clear *M*-H hysteresis loop indicates that the films exhibit room temperature ferromagnetism. It has been reported that the magnetic properties of various ternary and binary alloy films as well as bi-layer films are strongly influenced by film surface roughness. The coercivity, saturation magnetization, and remanent magnetization increase with an increase in surface roughness [34–36]. These magnetic parameters along with the magnetic anisotropy constant also vary with in-situ and post-annealing conditions of the films [11, 13]. In our results, the alloy film of 26% Ni has saturation magnetization of 194 emu/cc, which decreases to 87 emu/cc for Ni 45% and again increases to 221 emu/cc for Ni 60%. On the other hand, the coercivity (H_C) of the thin film with 26% Ni is found to be 49 Oe which increases to 92 Oe for the film with 45% Ni and 59 Oe for the film with 60% Ni. The variation of surface roughness parameters and RT magnetic parameters of thin films with Ni content is presented in Fig. 7. Though M_S and H_C vary with film composition, the variation is irregular as seen in Fig. 7. (a) and (b). However, the variation of M_S and H_C are found to be in accordance with the variation of S_a and R_a of these films. H_C increases with an increase in S_a of the films systematically (Fig. 7. (c)). On the other hand, the value of M_S first increases slightly with S_a and then decreases drastically with a further increase in S_a. The films with greater S_a and R_a possess the

Table 1
Film thickness, average film surface roughness estimated by 3D optical profilometer and RT magnetic parameters M_S and H_C of $Co_{1-x-y}Tb_xNi_y$ thin films.

Sl No.	Film composition	Thickness (nm)	Average Surface Roughness		Magnetic Parameters	
			S_a (nm)	R_a (nm)	M_S (emu/cc)	H_C (Oe)
1	$Co_{0.63}Tb_{0.11}Ni_{0.26}$	120	1.083	0.463	194	49
2	$Co_{0.41}Tb_{0.14}Ni_{0.45}$		1.632	0.735	87	92
3	$Co_{0.32}Tb_{0.08}Ni_{0.60}$		1.376	0.487	221	59

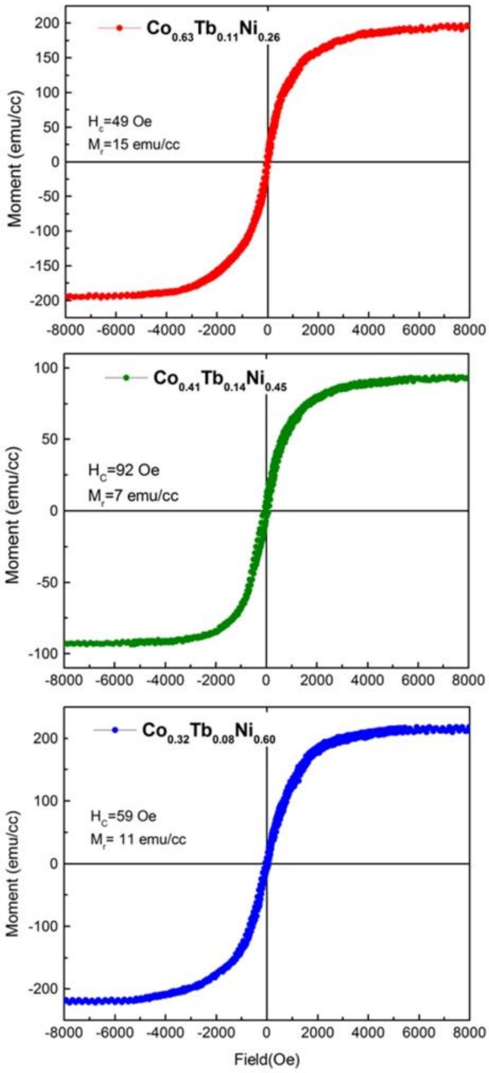

Fig. 6. Room temperature *M*-H loop of annealed $Co_{1-x-y}Tb_xNi_y$ alloy thin films.

greater values of H_C and smaller M_S which may be due to the contribution of domain wall pinning induced by film surface roughness and grain size [52]. A similar variation of H_C and other magnetic parameters such as M_S, anisotropy constant, etc., as a function of surface roughness, has also been reported in many other thin films [52–54]. These observations indicate that surface roughness dominates the influence of film composition in controlling the magnetic properties of these thin films. This is due to the fact that higher film surface roughness can produce inhomogeneous surface features and defects which then act as pinning centers impeding the domain wall motion as described by Zhao et al. in their theoretical calculations [55].

4. Conclusion

In conclusion, we have prepared $Co_{1-x-y}Tb_xNi_y$ ternary alloy thin films by co-sputtering of $Co_{0.85}Tb_{0.15}$ alloy target and pure Ni target using a dc magnetron sputtering system. The deposited thin films are found to be uniform and homogeneous as indicated by the

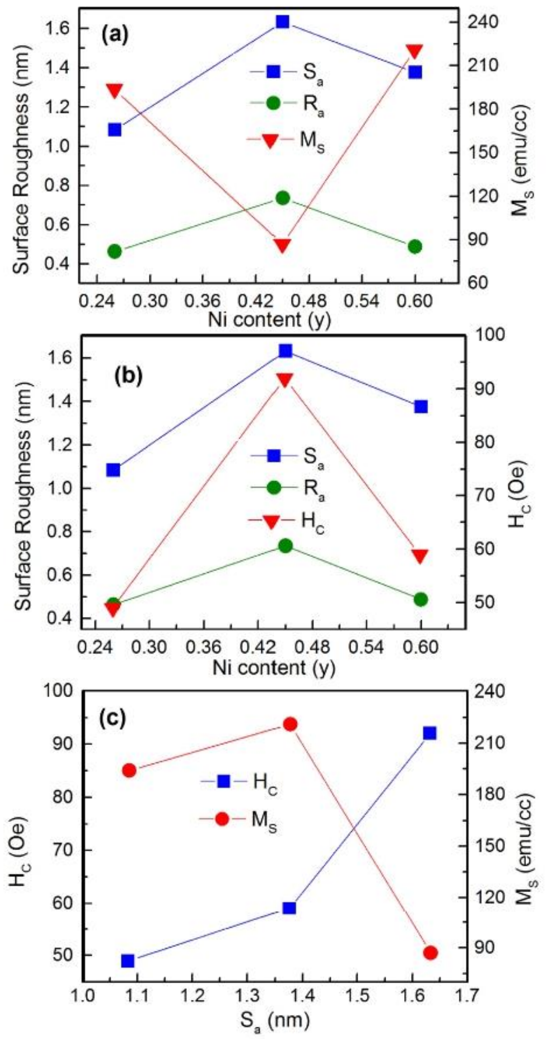

Fig. 7. Comparative plot of the variation of (a) S_a, R_a, and H_C, (b) S_a, R_a and M_S as a function of Ni-content, and (c) H_C and M_S as a function of S_a of $Co_{1-x-y}Tb_xNi_y$ alloy thin films.

elemental colour mapping spectra of EDS. The Ni content and roughness (S_a and R_a) of the films vary with sputtering target voltage. The deposited thin films are crystallized in amorphous form as confirmed by XRD measurement. All the alloy thin films exhibit RT ferromagnetism as confirmed by RT *M*-H hysteresis curve measurement. The magnetic parameters H_C and M_S vary with both film composition and film surface roughness. The nature of variation of H_C and M_S suggests that the magnetic properties of these amorphous alloy thin films are strongly correlated to film surface roughness. The observed results show that the film surface roughness along with film composition also plays significant role in tuning the magnetic properties.

Author Statements

R. K. Basumatary: Investigation, Methodology, Formal analysis, Writing Manuscript; P. Behera: Investigation; B. Basumatary: Investigation; B. Brahma: Investigation; S. Ravi: Writing – review & editing; S. Ravi: Resources, Writing – review & editing; R. Brahma: Visualization, Resources, Writing – review & editing, Supervision; S. K. Srivastava: Conceptualization, Methodology, Visualization, Writing – review & editing, Supervision.

Declaration of competing interest

The authors declare that they have no known competing financial interests or personal relationships that could have appeared to influence the work reported in this paper.

Data availability

Data will be made available on request.

References

[1] A. Chiu, I. Croll, D.E. Heim, R.E. Jones Jr., P. Kasiraj, K.B. Klassen, C.D.R.G. Simmons, IBM J. Res. Dev. 40 (1996) 283–300.
[2] P.C. Andricacos, N. Robertson, IBM J. Res. Dev. 42 (1998) 671–680.
[3] E.J. O'Sullivan, E.I. Cooper, L.T. Romankiw, K.T. Kwietniak, P.L. Trouilloud, J. Horkans, C.V. Jahnes, I.V. Babich, S. Krongelb, S.C. Hegde, J.A. Tornello, N. C. LaBianca, J.M. Cotte, T.J. Chainer, IBM J. Res. Dev. 42 (1998) 681–694.
[4] C. Liu, T. Tsao, G.-B. Lee, J.T.S. Leu, Y.W. Yi, Y.-C. Tai, C.-M. Ho, Sens. Actuators, A 78 (1999) 190–197.
[5] F.E. Rasmussen, J.T. Ravnkilde, P.T. Tang, O. Hansen, S. Bouwstra, Sens. Actuators, A 92 (2001) 242–248.
[6] K. Umadevi, S. Bysakh, J.A. Chelvane, S.V. Kamat, V. Jayalakshmi, J. Alloys Compd. 663 (2016) 430–435.
[7] T. Osaka, M. Takai, K. Hayashi, K. Ohashi, M. Saito, K. Yamada, Nature 392 (1998) 796–798.
[8] X. Liu, G. Zangari, L. Shen, J. Appl. Phys. 87 (2000) 5410–5412.
[9] K. Hironaka, S. Uedaira, IEEE Trans. Magn. 26 (1990) 2421–2423.
[10] B. Brahma, Pratap Behera, S. Ravi, R. Brahma, S.K. Srivastava, Appl. Phys. A 127 (2021) 680.
[11] B. Brahma, R. Hussain, , Aakansha, P. Behera, S. Ravi, R. Brahma, S.K. Srivastava, Thin Solid Films 728 (2021), 138689.
[12] R. Hussain, , Aakansha, S. Ravi, S.K. Srivastava, Solid State Commun. 324 (2021), 114144.
[13] R. Hussain, , Aakansha, S. Ravi, S.K. Srivastava, J. Mater. Sci. Mater. Electron. 31 (2020) 11975–11982.
[14] R.K. Basumatary, , Aakansha, B. Basumatary, B. Brahma, R. Hussain, S. Ravi, R. Brahma, S.K. Srivastava, J. Supercond. Nov. Magnetism 33 (10) (2020) 3165–3170.
[15] B. Brahma, R. Hussain, R.K. Basumatary, S. Ravi Aakansha, R. Brahma, S.K. Srivastava J, Supercond. Novel Magn. 33 (9) (2020) 2891–2897.
[16] R. Hussain, , Aakansha, B. Brahma, R. Basumatary, R. Brahma, S. Ravi, S.K. Srivastava, J. Supercond. Nov. Magnetism 33 (6) (2020) 1759–1763.
[17] T. Hauet, L. Piraux, S.K. Srivastava, V.A. Antohe, D. Lacour, M. Hehn, F. Montaigne, J. Schwenk, M.A. Marioni, H.J. Hug, O. Hovorka, A. Berger, S. Mangin, F. Abreu, Araujo Phys. Rev. B 89 (2014), 174421.
[18] L. Piraux, V. Antohe, F.A. Araujo, S.K. Srivastava, M. Hehn, D. Lacour, S. Mangin, T. Hauet, Appl. Phys. Lett. 101 (2012), 013110.
[19] I.A. Campbell, J. Phys. F Met. Phys. 2 (1972) L47.
[20] P. Hansen, C. Clausen, G. Much, M. Rosenkranz, K. Witter, J. Appl. Phys. 66 (1989) 756–767.
[21] H. Takagi, S. Tsunashima, S. Uchiyama, J. Appl. Phys. 50 (2008) 1642–1644.
[22] T. Niihara, S. Takayama, Y. Sugita, IEEE Trans. Magn. **MAG**- 21 (1985) 1638–1640.
[23] S. Miyanishi, K. Kojima, J. Sato, K. Takayama, H. Fuji, A. Takahashi, K. Ohta, J. Appl. Phys. 93 (2003) 7801–7803.
[24] H. Ito, K. Song, M. Naoe, J. Appl. Phys. 79 (1996) 6273–6275.
[25] J. Sato, Y. Murakami, H. Fuji, K. Kojima, A. Takahashi, R. Nakatani, M. Yamamoto, Jpn. J. Appl. Phys. 47 (2008) 150–153.
[26] Y.H. Fang, P.C. Kuo, C.Y. Chou, S.C. Chen, N.W. Cheng, P.L. Lin, J. Magn. Magn Mater. 310 (2007) e930–e932.
[27] M.T. Rahman, X. Liu, A. Morisako, J. Magn. Magn Mater. 303 (2006) e133–e136.
[28] K. Moorjani, J.M.D. Coey, Magnetic Glasses, Elsevier, Amsterdam, 1984, pp. 210–218.
[29] P. Hansen, in: K.H.J. Buschow (Ed.), Handbook of Magnetic Materials, vol. 6, Elsevier, Amsterdam, 1991, pp. 315–319.
[30] R. Hussain, B. Aakansha, Brahma, R.K. Basumatary, R. Brahma, S. Ravi, S.K. Srivastava, J. Supercond. Nov. Magnetism 32 (2019) 4027–4031.
[31] S.K. Srivastava, R. Hussain, T. Hauet, L. Piraux, AIP Conf. Proc. 2115 (2019), 030482.
[32] M. Tang, S. Chen, X. Zhang, Z. Zhang, Q.Y. Jin, Spin 6 (2016), 1650009.
[33] H. Fu, M. Mansuripur, P. Meystre, Phys. Rev. Lett. 66 (1991) 1086.
[34] Y. Cao, C. Zhou, J. Magn. Magn Mater. 333 (2013) 1–7.
[35] J. Swerts, K. Temst, N. Vandamme, C. Van Haesendonck, Y. Bruynseraede, J. Magn. Magn Mater. 240 (2002) 380–382.
[36] C.E. Davies, R.E. Somekh, J.E. Evetts, Vacuum 38 (1988) 797–800.
[37] W. Zhou, C.T. Ma, T.Q. Hartnett, P.V. Balachandran, S.J. Poon, AIP Adv. 11 (2021), 015334.
[38] H. Basumatary, J. Arout Chelvane, D.V. Sridhara Rao, S.V. Kamat, R. Ranjan, J. Magn. Magn Mater. 384 (2015) 58–63.
[39] J. Swerts, K. Temst, M.J. Van Bael, C. Van Haesendonck, Y. Bruynseraede, Appl. Phys. Lett. 82 (2003) 1239.
[40] S. Vilain, J. Ebothe, M. Troyon, J. Magn. Magn Mater. 157/158 (1996) 274–275.
[41] J. Sato, Y. Murakami, H. Fuji, K. Kojima, A. Takahashi, R. Nakatani, M. Yamamoto, Jpn. J. Appl. Phys. 47 (2008) 150–153.
[42] C.M. Lee, L.-X. Ye, J.-M. Lee, W.L. Chen, C.Y. Huang, G. Chern, T.H. Wu, IEEE Trans. Magn. 45 (2009) 3808–3811.
[43] H. Katayama, K. Watanabe, K. Takayama, J. Sato, S. Miyanishi, K. Kojima, K. Ohta, Appl. Phys. Lett. 81 (2002) 4994.
[44] L.-X. Ye, R.C. Bhatt, C.-M. Lee, W.-H. Hsu, T.H. Wu, J. Magn. Magn Mater. 502 (2020), 166554.
[45] S.Q. Yin, X.Q. Li, X.G. Xu, J. Miao, Y. Jiang, IEEE Trans. Magn. 47 (2011) 3129–3131.
[46] L.-X. Ye, C.-M. Lee, J.-M. Lee, W.-L. Tseng, T.H. Wu, IEEE Trans. Magn. 48 (2012) 2820–2822.
[47] M. Tang, S. Chen, X. Zhang, Z. Zhang, Q.Y. Jin, Spin 6 (2016), 1650009.
[48] A. Talapatra, J. Arout Chelvane, J. Mohanty, J. Magn. Magn Mater. 448 (2018) 360–366.
[49] K. Wang, S. Dong, Y. Huang, Y. Qiu, J. Magn. Magn Mater. 434 (2017) 169–173.
[50] F. Rafieian, M. Mousavi, A. Dufresne, Q. Yu, Int. J. Biol. Macromol. 164 (2020) 4444–4454.
[51] K. Sin, J.M. Sivertsen, J. Appl. Phys. 75 (1994) 5972.
[52] G. Choe, M. Steinback, J. Appl. Phys. 85 (1999) 5777.
[53] K. Matsuki, F. Kogiku, N. Morito, IEEE Trans. Magn. 34 (1998) 1180–1182.
[54] S. Vilain, J. Ebothe, M. Troyon, J. Magn. Magn Mater. 157/158 (1996) 274–275.
[55] Y.-P. Zhao, R.M. Gamache, G.-C. Wang, T.-M. Lu, J. Appl. Phys. 89 (2001) 1325.

Conference Certificates

National Conference on
Advances in Sustainable Chemistry and Material Science
(ASCMS-2022)

ASCMS

Paper Presentation Certificate

This is to certify that

Prof./Dr./Mr./Ms. *Rajib Kumar Basumatary* of *Bodoland University, Kokrajhar* has made oral presentation on the topic entitled "*3D Surface Topography and Surface Roughness measurement of CoTb based RE-TM ternary Alloy Thin Films - - - - - - .*" in the National Conference on Advances in Sustainable Chemistry and Material Science-2022 held on 29th & 30th April 2022 in the Department of Chemistry, Bodoland University, Kokrajhar, Assam, India.

Prof. Laishram Ladu Singh (Vice Chancellor)	Dr. Manjil Basumatary (Chairperson)	Dr. Sanjay Basumatary (Convenor)	Dr. Dhrubajyoti Haloi (Convenor)	Dr. Hem Prabha Saikia (Convenor)

XIII Biennial National Conference of Physics Academy of North East
(PANE-2022)
Department of Physics, Manipur University
08-10 November, 2022

PANE

CERTIFICATE OF PARTICIPATION

This is to certify that Rajib Kumar Basumatary, Assistant Professor/Ph.D. Scholar of Darrang College/Bodoland University has presented a paper entitled Surface Topography and Surface Roughness Study of CoTbNi Alloy Thin Films using 3D Optical Profilometer in the XIII Biennial National Conference of Physics Academy of North East (PANE-2022) held on 8-10 November, 2022 organized by the Department of Physics, Manipur University, Imphal-795003, Manipur, India.

Dr. Th. Gomti Devi Convenor Local Organizing Committee, MU	Prof. Ng. Nimai Singh President, PANE	Prof. H. Basantakumar Sharma Chairman HOD, Department of Physics, MU

Activa